# Expanding Naloxone Accessibility: A Lifesaver or a Risky Setback?

Junyang Cai*, Noa Zychlinski
Faculty of Data and Decision Science, Technion – Israel Institute of Technology, Haifa, 3200003, Israel,
junyang.cai@campus.technion.ac.il, noazy@technion.ac.il

The widespread prevalence of opioids has prompted governments to implement targeted interventions aimed at reducing overdose mortality, with naloxone accessibility emerging as one of the most prominent policies. Naloxone, a potent opioid antagonist, is highly effective in reversing overdoses, yet its expanded availability introduces complex trade-offs, particularly in the presence of moral hazard.

We develop a dynamic compartmental model that captures transitions between susceptible individuals and those with opioid use disorder (OUD), allowing us to evaluate the impact of naloxone accessibility on overdose mortality and to derive the optimal accessibility policy. We show that full naloxone accessibility is optimal in the absence of moral hazard or when its effect is small. However, when moral hazard is significant—where greater access to naloxone encourages riskier opioid use—expanded accessibility can paradoxically increase overdose deaths.

Extending the model to incorporate peer-driven contagion in opioid misuse, we find that the structure of the optimal policy remains robust, preserving the bang-bang nature and the reversal induced by moral hazard. Two additional insights emerge under this interaction-based model. First, in epidemics primarily driven by prescription-induced opioid use, full accessibility remains optimal. In contrast, when opioid use spreads socially—especially as the effectiveness of naloxone declines due to potent synthetic opioids like carfentanil—limited accessibility may become preferable. Second, the relationship between naloxone accessibility and overdose mortality may become non-monotonic, exhibiting an inverted U-shape in which moderate increases in accessibility can initially worsen outcomes.

A calibrated case study based on U.S. data suggests that under current epidemic conditions, full accessibility remains optimal—a finding that aligns with existing regulatory policies. However, our results highlight that shifts in epidemic dynamics, such as increased opioid potency, may fundamentally alter this conclusion. These findings underscore the need for continuous reevaluation of naloxone distribution policies as the opioid crisis evolves.

*Key words*: opioid epidemic, naloxone accessibility, moral hazard, mathematical model, healthcare management

*History*: Received: August 2024; accepted: November 2025 by Sergei Savin after three revisions.

* Corresponding Author

## 1. Introduction

The opioid epidemic is a growing global crisis, with the U.S. experiencing particularly severe impacts. Prescription opioids—such as tramadol and medical fentanyl—are widely used for pain relief but are highly susceptible to misuse, leading to dependency and addiction. For individuals who overdose, the risk of respiratory depression is significant, and without the timely administration of the opioid antagonist naloxone, the likelihood of suffocation and death rises dramatically.

A 2019 investigation from the World Health Organization (2024) reported that approximately 600,000 people worldwide died from drug-related causes, with nearly 80% of those deaths attributed to opioids. Moreover, the opioid epidemic in the U.S. worsened during the COVID-19 pandemic, as many individuals turned to illicit synthetic fentanyl to cope with mental health issues such as anxiety and depression (Haley and Saitz 2020, Abramson 2021). According to the National Institute on Drug Abuse (2024), the annual number of deaths related to opioid overdoses in the U.S. was approximately 50,000 between 2017 and 2019, surged to 68,630 in 2020, and further increased to 81,806 in 2022.

The staggering number of deaths poses a grave threat to public health and well-being, making it imperative for governments to implement policies aimed at reducing opioid-related mortality. One direct approach is to enhance the accessibility of naloxone, enabling individuals to promptly administer this life-saving medication in the event of an overdose. Specifically, classifying naloxone as a non-prescription medicine and allowing individuals with opioid use disorder (OUD) to take it home has helped increase access (Hardin et al. 2024). Several countries have adopted such measures in recent years. In 2023, the U.S. Food and Drug Administration (FDA) approved Narcan, a nasal spray form of naloxone, for over-the-counter (OTC) use, allowing purchase without a prescription. Canada and Australia implemented similar policies in 2016 and 2022, respectively, and Sweden is preparing to follow suit (Euractiv 2024).

Despite these advances, important questions remain about the unintended consequences and broader systemic effects of naloxone accessibility. Two key mechanisms underlie this complexity: *moral hazard* and *social contagion*.

*Moral hazard.* Expanding naloxone access may inadvertently encourage riskier opioid use by changing the perceived consequences of overdose. For instance, Sally Satel, a psychiatrist and drug policy scholar, noted, *"Patients occasionally tell me that having naloxone on hand has served as insurance against overdose. So, in some instances, it enhances risk taking"* (The Washington Post 2018). Empirical findings on this channel are mixed—some studies detect increases in risky use or treatment episodes following access expansions, while others find little or no change (Ardeljan et al. 2023, Qayyum et al. 2023). These competing narratives highlight the need to assess whether and when moral hazard meaningfully offsets naloxone's life-saving potential.

*Social contagion.* Heterogeneous outcomes across regions also suggest the importance of social and geographic networks. Opioid use and overdose risk can concentrate and spread through such networks: peers transmit norms and information, supply and potency shocks move along shared connections, and changes in local services spill over to nearby communities (Adamopoulou et al. 2024, Seamans et al. 2018). These social dynamics can amplify or dampen the impact of access policies, implying that naloxone's effectiveness depends not only on individual behavior but also on the structure of interactions within affected populations.

Taken together, these motivations raise two central research questions: (1) How does expanding naloxone accessibility affect overdose mortality once behavioral responses and social spillovers are accounted for? (2) What level of accessibility minimizes opioid-related deaths across different environments? To answer these questions, we develop and analyze a sequence of models that explicitly incorporates the relationship between naloxone accessibility, overdose mortality, and the emergence of new individuals with OUD, while accounting for both moral hazard and peer-driven contagion in opioid misuse. Our framework treats access as a policy lever, quantifies when it remains beneficial versus when it can backfire, and yields structured, testable policy guidance. Despite the urgency and societal relevance of this issue, it remains largely underexplored in the operations research and operations management literature.

Specifically, we introduce a mathematical framework that combines a Susceptible–Addicted–Susceptible (SAS) structure with explicit modeling of naloxone accessibility as an optimizable policy variable. The framework is organized as a four-model cascade: a baseline SAS model, an extension with moral hazard (SAS-M), an extension with social contagion (D-SAS), and a combined model with both mechanisms (D-SAS-M). This design captures the dynamic interplay between opioid use, overdose mortality, and behavioral responses, enabling us to evaluate trade-offs between overdose prevention and risk compensation. We also complement the analytical results with a calibrated U.S. case study, which assesses current epidemic conditions and explores how future changes in opioid potency could reverse policy conclusions.

The paper makes the following key contributions:

- ***An operational modeling framework for naloxone accessibility.*** We introduce a mathematical framework to analyze the opioid crisis, combining a Susceptible–Addicted–Susceptible (SAS) structure with explicit modeling of naloxone accessibility as a policy lever that can be optimized. The framework consists of four models—a baseline SAS model, an extension with moral hazard (SAS-M), an extension with social contagion (D-SAS), and a combined model with both mechanisms (D-SAS-M). This setup captures the dynamic interplay between opioid use, overdose mortality, and behavioral responses, allowing systematic evaluation of the trade-offs between overdose prevention and potential risk compensation.

- ***Structured characterization of optimal accessibility under moral hazard.*** We formulate and solve an optimization problem that minimizes overdose mortality while explicitly accounting for moral hazard, where greater accessibility may encourage riskier opioid consumption. The analysis provides a transparent policy rule that links behavioral responses to the recommended level of access and identifies when more limited accessibility may become preferable. While policymakers are aware of this trade-off, our model formalizes it and provides an interpretable threshold-style guideline that can inform ongoing policy evaluation.
- ***Robustness of optimal policy under social contagion dynamics.*** We show that the structure of the optimal policy remains robust even when incorporating peer-driven contagion in opioid misuse. The switching behavior identified under moral hazard persists, but social dynamics can generate additional complexity, including a non-monotonic (inverted U-shaped) relationship between accessibility and mortality.
- ***Empirical calibration and case study.*** We calibrate the framework using U.S. data to assess current epidemic conditions. The analysis suggests that full public accessibility remains optimal under present circumstances but may reverse as opioid potency increases, underscoring the importance of continuous policy reassessment.

The remainder of the paper proceeds as follows. Section 2 reviews the related literature. Sections 3–6 sequentially develop the four models and analyze the resulting policy implications. Section 7 presents a calibrated U.S. case study, and Section 8 concludes with implications and future research directions. Technical proofs appear in the electronic companion.

## 2. Literature Review

Our work relates to three research streams: (1) operations research/operations management (OR/OM) studies of the opioid crisis; (2) epidemiological models of overdose and substance use; and (3) naloxone-policy debates in economics, public health, and medicine.

### 2.1. The Opioid Crisis in OR/OM

Early OR/OM work on addiction management includes Zaric et al. (2000), who analyzed the U.S. drug crisis and showed that expanding methadone maintenance is cost-effective and improves outcomes for injection drug users. Although academic attention waned for a period, interest has grown markedly in recent years.

A central operational challenge is the extremely short "golden window" in which naloxone can reverse an overdose. To reach individuals who do not have naloxone on hand, recent studies design drone networks for rapid delivery: Gao et al. (2024) and Lejeune and Ma (2025) formulate optimization models that reduce response time and mortality. Other work integrates epidemic dynamics with resource allocation: Ansari et al. (2024) couples a dynamic compartmental model

with a Markov decision process to optimize budgets across interventions, and Luo and Stellato (2024) links a dynamic model with a mixed-integer program to improve treatment-facility siting and budgeting, thereby expanding access for people with OUD. Baucum et al. (2025) proposed a predict-then-optimize framework to reallocate treatment centers across U.S. counties, balancing mortality reduction with equity. In related work, Gökçınar et al. (2022) developed a prescription opioid pain management framework to balance pain relief and addiction risk, and Bertsimas et al. (2025) presented a semisupervised machine learning approach to detect illegal diversion in the U.S. prescription opioid supply chain. Building on this stream, Gan et al. (2025) introduce a constrained partially observable Markov decision process that leverages wearable data to optimize personalized OUD treatment strategies.

Complementing these model-driven studies, several OM papers take empirical approaches to the opioid/drug crisis. For example, Yang and Mishra (2025), Liu and Bharadwaj (2020), Bobroske et al. (2022), KC et al. (2022), and Attari et al. (2025) examine how factors such as online platforms, supply-chain practices, and race correlate with opioid/drug-related outcomes, yielding evidence to guide management and policy.

Despite this progress, to our knowledge, there are no analytical models that explicitly link naloxone accessibility to epidemic dynamics and that optimize its availability. We address this gap by developing and analyzing stylized mathematical models that clarify the managerial and policy implications of naloxone accessibility—an issue of urgent public-health and societal importance.

### 2.2. Epidemiological Models of Overdose and Substance Use

Rooted in infectious-disease epidemiology, compartmental models use systems of differential equations to track population movements—e.g., initiation, casual or nonmedical use, OUD, treatment, recovery, and relapse—while incorporating overdose risk as a (potentially state-dependent) hazard. Related methodologies have been applied to forecast outbreaks and design allocation policies in public health (e.g., Zhou et al. 2025, Li et al. 2023).

Unlike OR/OM studies that embed these dynamics for resource allocation, this subsection focuses on the epidemiological structure and its implications for overdose. In biomathematics, compartmental models of the opioid crisis are widely studied. For example, Battista et al. (2019) incorporate prescription-induced initiation and treatment; Cole et al. (2024) add a saturation treatment function and an explicit casual-user class; and additional work analyzes heroin-use dynamics and related mechanisms (Djilali et al. 2017, Huang and Liu 2013, Cole and Wirkus 2022). Collectively, these models clarify how initiation, social influence, treatment capacity, and relapse interact to shape prevalence and overdose mortality.

Our SAS family of models fits squarely within this epidemiological tradition: it captures prescription-induced initiation, socially contagious addiction, and explicit overdose hazards, yet

remains analytically tractable and yields closed-form equilibria. Moreover, we model moral hazard and the role of naloxone accessibility within the dynamical system, providing interpretable thresholds and comparative statics that connect epidemiological mechanisms to actionable policy insights.

### 2.3. Naloxone Policy Across Economics, Public Health, and Medicine

Across economics, public health, and medicine, naloxone accessibility remains the subject of active debate. A large public health and clinical literature supports expanding access. For example, Rao et al. (2021) project that overdose deaths in the U.S. could reach 1,220,000 by 2029 and estimate that a 30% increase in naloxone access would avert roughly 25% of these deaths. Jawa et al. (2022) advocate broader access and over-the-counter availability, including insurer reimbursement for people with OUD; similar recommendations appear in Burris et al. (2009), Houser (2023), Messinger et al. (2023), Saberi et al. (2024).

In contrast, several economic studies emphasize behavioral responses—often framed as moral hazard—where protection from harm can induce riskier behavior (e.g., Doleac and Mukherjee 2022, Packham 2022). The classic illustration comes from traffic safety, where improvements were argued to offset some benefits via riskier driving (Peltzman 1975); analogous mechanisms have been discussed in finance and insurance, where government guarantees may encourage risk-taking (Pernell and Jung 2024).

Applied to opioids, Doleac and Mukherjee (2022) and Packham (2022) argue that expanding naloxone access may yield mixed effects if it unintentionally encourages riskier use. Related evidence shows that certain decriminalization policies—by increasing drug accessibility—were followed by unexpected rises in overdose deaths (Spencer 2023, Liu et al. 2025). Our findings also connect to Cawley and Dragone (2024), who show that introducing less harmful substitutes (e.g., methadone) can improve outcomes but, under some conditions, may generate unintended consequences.

Taken together, our contribution to this debate is to frame naloxone access as an operational policy choice embedded in epidemiological dynamics. The model delivers transparent, threshold-based policy rules and testable predictions (e.g., potential inverted-U effects and regime switches as behavioral response or contagion intensifies) that help reconcile mixed empirical findings. It also guides measurement—estimating behavioral responses, transmission intensity, and overdose lethality across low- and high-risk states—to enable continuous re-evaluation. A calibrated U.S. case study indicates that full access is currently optimal, while the same framework pinpoints conditions (e.g., more frequent overdoses or reduced reversal effectiveness) under which limited public access would minimize deaths.

## 3. The Basic SAS Model

Our basic SAS model, illustrated in the top-left panel of Figure 1, comprises two groups: $S(t)$, the number of susceptible individuals at time $t$, and $A(t)$, the number of individuals with OUD at time $t$.

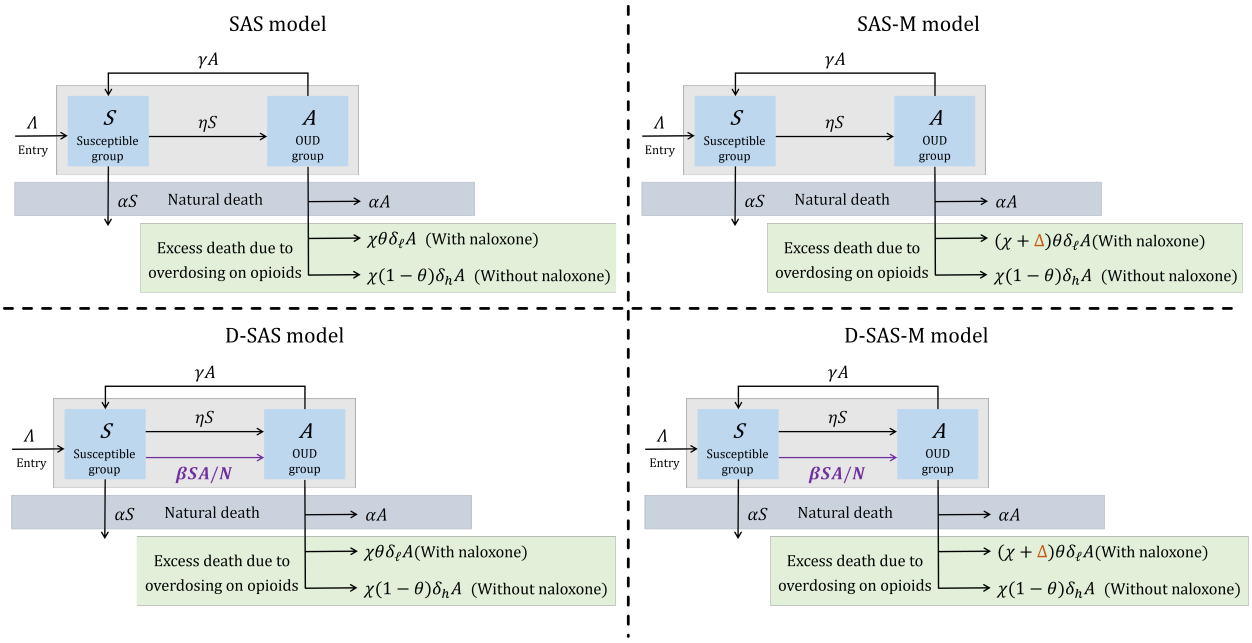


**Figure 1** **Illustration of the four-model SAS cascade (SAS, SAS-M, D-SAS, and D-SAS-M).**

We denote by $\Lambda > 0$ the inflow rate into the susceptible group, and by $\alpha > 0$ the natural death rate representing outflow from both groups. Similar to Luo and Stellato (2024), in our basic model, we assume that new individuals with OUD are generated at a transition rate $\eta > 0$ from the susceptible group. This transition pattern can be interpreted as patients spontaneously developing OUD as a result of opioid prescription induction.

In the case of an overdose, $\delta_\ell \in (0,1)$ and $\delta_h \in (0,1)$ denote the mortality rates at the individual level, with $\delta_\ell$ being lower when timely treatment with naloxone is provided, and $\delta_h$ being higher when such treatment is unavailable. That is, $\delta_h > \delta_\ell$. The rate at which overdose events occur among individuals with OUD is denoted as $\chi > 0$.

**Decision variable.** We let $\theta \in [0,1]$ denote naloxone accessibility delivered through population-level *public* channels (standing orders, public distribution), defined as the share of individuals with OUD who have naloxone available at the time of an overdose. Thus, $\theta$ is both the policy lever and the corresponding possession share: $\theta = 1$ represents public access sufficient to yield (near-)universal immediate access, whereas $\theta = 0$ means public channels are not in operation. Importantly, $\theta = 0$

does not imply clinical unavailability; strict prescription and clinician-administered use remain possible.

Indeed, clinician-mediated access remains possible even when public channels are off. A parallel exists in other regulatory contexts: in the U.S., methamphetamine is a Schedule II controlled substance—nonmedical distribution is illegal, yet limited medical use under strict supervision is permitted (Drug Enforcement Administration 2025).

While our model primarily focuses on naloxone accessibility for individuals with OUD, we acknowledge that expanding naloxone access extends beyond this group to the general public. By increasing community-wide availability, policymakers aim to ensure that bystanders can intervene during an overdose, reinforcing the broader public health objective of reducing opioid-related mortality across society.

Lastly, we denote by $\gamma > 0$ the rate at which individuals with OUD successfully overcome their active use through medication-assisted treatment or other therapeutic methods. Recognizing the potential for relapse, we also account for individuals who, after successful detoxification, may revert to active use.

In the basic model, we assume that opioid overdose rates are uniform across the OUD population, regardless of naloxone possession. In other words, possessing naloxone does not lead to increased opioid consumption or overdose. This assumption aligns with a widely accepted perspective within parts of the public health community (New York Times 2024, Tse et al. 2022). In Section 4, we incorporate a moral hazard, which suggests an increased risk of opioid overdose among individuals with OUD who possess naloxone, as argued by some economic studies (Doleac and Mukherjee 2022, Packham 2022).

Furthermore, in Section 5 and Section 6, we introduce two model extensions in which the generation of new individuals with OUD could be influenced by interactions between the susceptible and OUD groups – an approach aligns with the framework of infectious model prevalent in epidemiology, which has been proposed in several studies as a suitable representation of the opioid overdose crisis (Ansari et al. 2024, Cole et al. 2024).

The dynamics of the basic SAS model are described by the following system of differential equations:

$$\begin{cases} \dot{S}(t) = \Lambda - (\alpha + \eta)\, S(t) + \gamma A(t), \\ \dot{A}(t) = \eta S(t) - (\alpha + \gamma + \chi\theta\delta_\ell + \chi(1-\theta)\delta_h)\, A(t), \\ S(t), A(t) \geq 0. \end{cases} \tag{1}$$

Note that the overall mortality rate regarding overdose in model (1) is $(\chi\theta\delta_\ell + \chi(1-\theta)\delta_h)$.

### 3.1. Optimization and Analysis

We begin by deriving the equilibrium point, $(S^*, A^*)$, for the basic model described in (1):

$$(S^*, A^*) = \left( \frac{\Lambda\left(\chi(\theta\delta_\ell + (1-\theta)\delta_h) + \alpha + \gamma\right)}{\alpha(\alpha+\gamma+\eta) + \chi(\alpha+\eta)(\theta\delta_\ell + (1-\theta)\delta_h)}, \frac{\eta\Lambda}{\alpha(\alpha+\gamma+\eta) + \chi(\alpha+\eta)(\theta\delta_\ell + (1-\theta)\delta_h)} \right).$$

Recognizing that fatal outcomes from opioid abuse represent the primary concern for both policymakers and society (CNN 2017, Reider 2019), our objective is to minimize the long-run average opioid overdose mortality. Specifically, we seek to solve:

$$\begin{aligned} \min_{\theta\in[0,1]} \quad \mathcal{D}(\theta) :=& \lim_{T\to\infty} \frac{1}{T} \int_0^T \chi(\theta\delta_\ell + (1-\theta)\delta_h) A(t)\, \mathrm{d}t \\ =& \chi(\theta\delta_\ell + (1-\theta)\delta_h) A^* \\ =& \frac{\eta\Lambda\chi(\theta\delta_\ell + (1-\theta)\delta_h)}{\alpha(\alpha+\gamma+\eta) + \chi(\alpha+\eta)(\theta\delta_\ell + (1-\theta)\delta_h)}. \end{aligned} \tag{2}$$

PROPOSITION 1 **(Optimal accessibility for the SAS model)**. *For problem (2), full naloxone accessibility is optimal.*

Proposition 1 establishes that full naloxone accessibility minimizes opioid overdose mortality. Intuitively, broader naloxone availability increases the likelihood of survival during overdose events among individuals with OUD. This result aligns with widely held views that advocate for universal access to naloxone (e.g., The Washington Post 2023). Furthermore, it is consistent with current FDA regulations, which support its approval as an OTC medication and emphasize the importance of maximizing its accessibility.

## 4. Accounting for Moral Hazard in SAS-M Model

While the basic SAS model establishes that full accessibility is optimal absent behavioral responses, real-world evidence suggests this may be incomplete (Doleac and Mukherjee 2022, Packham 2022). The *moral hazard* phenomenon, also known as the *Peltzman effect* (Peltzman 1975), has been widely discussed in relation to the opioid crisis. Moral hazard is an economic concept describing the tendency of individuals to take riskier actions when they can mitigate or avoid the consequences of those risks. A classic and illustrative example of moral hazard pertains to traffic safety: for instance, Sagberg et al. (1997) observed that taxi drivers operating vehicles equipped with Anti-lock Braking Systems (ABS) tend to wear seatbelts less frequently compared to those driving taxis without ABS.

In the context of the opioid crisis, there is growing concern that easier access to naloxone may encourage riskier opioid consumption behavior among individuals with OUD, leading to higher misuse rates. Specifically, individuals may consume opioids in a compensatory manner, assuming

naloxone will mitigate the risk of fatal overdose. Some economic studies have used econometric methods to provide evidence of moral hazard in this context (Doleac and Mukherjee 2022, Packham 2022). Furthermore, individuals who overdose and are revived with naloxone often experience severe withdrawal symptoms, which can increase the likelihood of immediate opioid reuse (Greene 2018).

However, some public health experts challenge these findings, arguing that moral hazard is either negligible or irrelevant in the context of the opioid crisis (New York Times 2024). They emphasize that the life-saving benefits of naloxone far outweigh the speculative risks of increased opioid misuse.

Since the existence and extent of moral hazard remain a subject of debate, we consider its potential impact on the opioid crisis and the optimal design of naloxone accessibility policies. Ignoring moral hazard risks may result in incomplete or suboptimal strategies for addressing opioid misuse and overdose fatalities. To this end, we introduce $\Delta \geq 0$ to capture moral hazard among individuals with OUD who have access to naloxone—an *additive term representing the elevated overdose rate* attributable to access, holding other drivers fixed (see the top-right panel of Figure 1). Thus, $\Delta = 0$ denotes no measurable risk compensation, whereas a positive $\Delta$ indicates that individuals with access face a higher baseline risk of overdose. For calibration, $\Delta$ is estimated using quasi-experimental evaluations of naloxone access laws (Abouk et al. 2019, Doleac and Mukherjee 2022) (see Section 7.1).

The SAS-M model incorporating *moral hazard* is in the following system of differential equations:

$$\begin{cases} \dot{S}(t) = \Lambda - (\alpha + \eta)\, S(t) + \gamma A(t), \\ \dot{A}(t) = \eta S(t) - (\alpha + \gamma + (\chi + \Delta)\delta_\ell \theta + \chi \delta_h (1-\theta))\, A(t), \\ S(t), A(t) \geq 0, \end{cases}$$

where $(\chi+\Delta)\delta_\ell\theta + \chi\delta_h(1-\theta)$ is the overall mortality rate regarding opioid overdose and $(\chi+\Delta)\delta_\ell\theta$ represents the mortality rate of the OUD group possessing naloxone at a moral hazard level $\Delta$. Clearly, there are additional $\Delta\delta_\ell\theta A(t)$ deaths involving opioids at time $t$.

### 4.1. Optimization and Analysis

We begin by deriving the equilibrium point $(S_M^*, A_M^*)$ for the SAS-M model:

$$(S_M^*, A_M^*) = \left( \frac{\Lambda\left(\alpha + \gamma + \chi(\theta\delta_\ell + (1-\theta)\delta_h) + \Delta\delta_\ell\theta\right)}{\alpha(\alpha+\gamma+\eta) + (\alpha+\eta)(\chi(\theta\delta_\ell + (1-\theta)\delta_h) + \Delta\delta_\ell\theta)}, \frac{\eta\Lambda}{\alpha(\alpha+\gamma+\eta) + (\alpha+\eta)(\chi(\theta\delta_\ell + (1-\theta)\delta_h) + \Delta\delta_\ell\theta)} \right).$$

The corresponding optimization objective for the SAS-M model is given by

$$\begin{aligned} \min_{\theta\in[0,1]} \mathcal{D}_M(\theta) &:= \lim_{T\to\infty} \frac{1}{T} \int_0^T \left(\chi(\theta\delta_\ell + (1-\theta)\delta_h) + \Delta\delta_\ell\theta\right) A(t)\, \mathrm{d}t \\ &= \left(\chi(\theta\delta_\ell + (1-\theta)\delta_h) + \Delta\delta_\ell\theta\right) A_M^* \\ &= \frac{\eta\Lambda\left(\chi(\theta\delta_\ell + (1-\theta)\delta_h) + \Delta\delta_\ell\theta\right)}{\alpha(\alpha+\gamma+\eta) + (\alpha+\eta)(\chi(\theta\delta_\ell + (1-\theta)\delta_h) + \Delta\delta_\ell\theta)}. \end{aligned} \tag{3}$$

As evident from (3), both the direct life-saving benefits of naloxone and the adverse effects of moral hazard contribute to overdose mortality through the term $\chi((1-\theta)\delta_h + \theta\delta_\ell) + \Delta\delta_\ell\theta$. In particular, for any fixed level of accessibility $\theta$, we have $\partial\mathcal{D}_M/\partial\Delta > 0$, indicating that an increase in moral hazard directly increases overdose mortality and may, therefore, contradict the public health objective of reducing overdose deaths.

To formally capture the tension between opposing forces from moral hazard and naloxone accessibility, we next define the neutral effect threshold associated with moral hazard:

$$\bar{\Delta} := \frac{\chi(\delta_h - \delta_\ell)}{\delta_\ell} > 0.$$

In other words, $\bar{\Delta}$ represents the critical threshold at which naloxone accessibility yields a neutral effect on overdose mortality. Specifically, when $\Delta = \bar{\Delta}$, the total overdose mortality rate, $(\chi + \bar{\Delta})\delta_\ell\theta + \chi\delta_h(1-\theta)$, simplifies to $\chi\delta_h$, which is independent of the accessibility level $\theta$.

Theorem 1 characterizes the optimal naloxone accessibility policy in the presence of moral hazard.

THEOREM 1 **(Optimal accessibility for the SAS-M model)**. *For problem (3), full accessibility is optimal if $\Delta < \bar{\Delta}$, and no accessibility is optimal otherwise.*

For clarity and consistency throughout the paper, the boundary case $\Delta = \bar{\Delta}$ is combined with the case where no accessibility is optimal. We note, however, that at this threshold, any accessibility yields identical overdose mortality levels and is therefore optimal. More generally, we classify any non-unique optimal policy that includes zero accessibility as a zero-accessibility policy by default throughout the paper.

According to Theorem 1, when moral hazard is relatively mild, the life-saving benefits of naloxone outweigh its adverse behavioral effects, making full accessibility optimal. Conversely, when moral hazard becomes sufficiently large, the negative consequences dominate, and restricting accessibility becomes preferable. Limiting access in this case helps mitigate overdose risk and prevents further loss of life. This bang-bang structure, in which the optimal policy lies at one of the extremes, is common in healthcare management models (Mehrez and Gafni 1987, Chehrazi et al. 2019).

Using the threshold in practice requires the estimation of $\Delta$ from quasi-experimental variation in access (see section 7.1). Compute the calibrated threshold $\bar{\Delta}$ and report a simple "distance to threshold". If the estimation value of $\Delta$ lies below the threshold, the model supports broad access; if above, more limited public access may be warranted.

Figure 2 illustrates the effect of naloxone accessibility on overdose mortality across varying levels of moral hazard. When moral hazard is relatively low ($\Delta < \bar{\Delta} = 0.06$), increasing naloxone accessibility leads to a decline in overdose mortality, highlighting the life-saving benefits of broader naloxone availability in settings with limited risk compensation behavior. In contrast, when moral

hazard is high ($\Delta > \bar{\Delta}$), greater naloxone accessibility results in *higher* overdose mortality, suggesting that excessive reliance on naloxone may encourage riskier opioid use behaviors that outweigh its protective effect. At the threshold level ($\Delta = \bar{\Delta}$), overdose mortality is independent of naloxone accessibility, indicating a tipping point at which the positive and negative effects of accessibility are balanced. Furthermore, holding naloxone accessibility $\theta$ constant, an increase in moral hazard consistently leads to higher overdose mortality, reinforcing the detrimental role of risk compensation in undermining public health interventions.

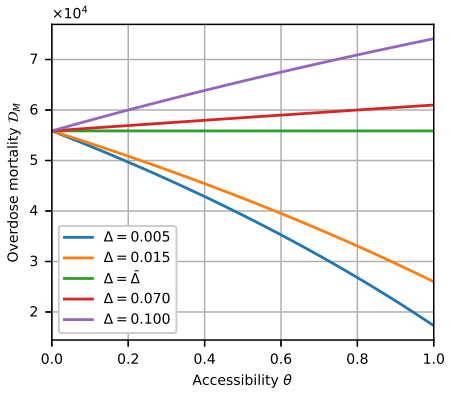


**Figure 2** **Naloxone accessibility effect on overdose mortality $\mathcal{D}_M$. The parameters are:** $\Lambda = 2 \times 10^5$, $\alpha = 0.01$, $\eta = 0.09$, $\chi = 0.012$, $\delta_h = 0.75$, $\delta_\ell = 0.125$, $\gamma = 0.1$, $\bar{\Delta} = 0.06$.

## 5. The D-SAS Model Incorporating Social Interaction

In this section, we extend the analysis by incorporating a peer-driven contagion mechanism, motivated by evidence that opioid use and overdose risk concentrate and spread through social and geographic networks (e.g., Battista et al. 2019, Cole and Wirkus 2022, Cole et al. 2024, Ansari et al. 2024). This perspective complements the infectious-disease analogy while making explicit the relevant channels: peer influence (norms and information), market linkages (shared supply and potency shocks), and service spillovers (changes in nearby harm-reduction or treatment access). In our formulation, the emergence of new cases depends on interactions between people at risk and those already affected, generating nonlinear growth consistent with observed clustering and diffusion patterns.

A substantial empirical literature documents peer, family, and neighborhood influences in opioid misuse and related outcomes. For example, Adamopoulou et al. (2024) show that serious injuries increase prescription exposure and the risk of misuse, which then spread through peer effects, raising a best friend's likelihood of opioid misuse by about 7%. Likewise, Seamans et al. (2018) find that exposure to a household member's opioid prescription increased the 1-year risk of subsequent

opioid use by 0.71% compared with exposure to a household member's nonopioid prescription. We therefore model social contagion explicitly and examine how these network-mediated effects interact with access policies in shaping overdose mortality.

We introduce the D-SAS model, illustrated in the bottom-left panel of Figure 1, which incorporates *dual* pathways for the pathogenesis of OUD: a constant-rate term, as in the baseline SAS model, and an interaction term that captures new cases arising from contacts between susceptible individuals and those with OUD. In Section 6, we further extend the model to include the effects of moral hazard.

We adopt the *standard incidence* form, $\beta\frac{S(t)A(t)}{N(t)}$, to model the interaction between susceptible individuals and individuals with OUD, where $\beta$ denotes the transmission rate, and $N(t)=S(t)+A(t)$ represents the total population at time $t$. This formulation is commonly used in epidemiological models of the opioid crisis (e.g., Cole and Wirkus 2022, Cole et al. 2024). The underlying assumption is that opioid transmission primarily occurs within localized and bounded social networks, where individuals tend to interact repeatedly within specific peer groups and communities (Mars et al. 2014). As a result, the likelihood of interaction depends on the proportion of individuals in each group rather than their absolute numbers (Martcheva 2015).

The D-SAS model is governed by the following system of differential equations:

$$\begin{cases} \dot{S}(t)=\Lambda-(\alpha+\eta)\,S(t)-\beta\dfrac{S(t)A(t)}{N(t)}+\gamma A(t), \\ \dot{A}(t)=\eta S(t)+\beta\dfrac{S(t)A(t)}{N(t)}-(\alpha+\gamma+\chi\theta\delta_\ell+\chi(1-\theta)\delta_h)\,A(t), \\ N(t)=S(t)+A(t),\ \ S(t),A(t)\geq 0. \end{cases} \tag{4}$$

Remark 1. To ensure the robustness of our results, we also analyze an alternative formulation based on the *mass action incidence* form, $\beta S(t)A(t)$, which has been used in previous studies of opioid use dynamics (e.g., Djilali et al. 2017, Huang and Liu 2013). The optimal accessibility policy for the D-SAS model under mass action incidence is provided in Appendix EC.1. While the solution formulations are slightly different, the overall structure of the solution and the key insights remain consistent, demonstrating the robustness of the results.

### 5.1. Optimization and Analysis

We denote the equilibrium of the D-SAS model by $(S_D^*, A_D^*)$, where closed-form expressions are provided in Appendix EC.2. The corresponding optimization problem aims to minimize the long-run average overdose mortality, given by:

$$\begin{aligned} \min_{\theta\in[0,1]} \quad \mathcal{D}_D(\theta) &:= \lim_{T\to\infty}\frac{1}{T}\int_0^T(\chi\theta\delta_\ell+\chi(1-\theta)\delta_h)\,A(t)\,\mathrm{d}t \\ &=\chi(\theta\delta_\ell+(1-\theta)\delta_h)A_D^*. \end{aligned} \tag{5}$$

Before characterizing the optimal naloxone accessibility policy for the D-SAS model in Theorem 2, we introduce the following auxiliary terms:

$$\bar{\beta} := \alpha + \gamma + \eta, \quad \bar{\delta} := \frac{\left(\beta - \bar{\beta}\right)^2 + 4\beta\eta}{2\chi\left(\beta - \bar{\beta}\right)}.$$

Note that $\bar{\delta} > 0$ when $\beta > \bar{\beta}$.

THEOREM 2 **(Optimal accessibility for the D-SAS model)**. *For problem (5), the optimal naloxone accessibility policy is as follows:*

1. ***Full accessibility is optimal*** *if any of the following conditions holds:*

a. $\beta \leq \bar{\beta}$;

b. $\beta > \bar{\beta}$ *and* $\delta_h \leq \bar{\delta}$;

c. $\beta > \bar{\beta}$, $\delta_\ell < \bar{\delta} < \delta_h$, *and* $\mathcal{D}_D(\theta = 1) < \mathcal{D}_D(\theta = 0)$.

2. ***No accessibility is optimal*** *if any of the following conditions holds:*

a. $\beta > \bar{\beta}$ *and* $\delta_\ell \geq \bar{\delta}$;

b. $\beta > \bar{\beta}$, $\delta_\ell < \bar{\delta} < \delta_h$, *and* $\mathcal{D}_D(\theta = 0) \leq \mathcal{D}_D(\theta = 1)$.

According to Theorem 2, the optimal accessibility level in the D-SAS model remains either full or zero. Full accessibility is optimal when the opioid crisis is primarily driven by spontaneous, prescription-induced addiction (Case 1a, i.e., when $\eta$ is relatively large), consistent with the results of the basic SAS model (Proposition 1).

In contagion-dominant environments (i.e., when $\beta > \bar{\beta}$), the optimal policy depends on the overdose rate $\chi$ to some degree. When $\chi$ is relatively low, the corresponding threshold $\bar{\delta}$ is large, making it more likely that $\delta_h \leq \bar{\delta}$ holds and that full accessibility remains optimal (Case 1b). In such settings, overdoses are infrequent, and expanding naloxone access enhances an already favorable situation by further reducing preventable deaths.

However, even when opioid misuse is largely driven by peer influence and social transmission, full accessibility may also no longer be optimal (Case 2). In these environments, preventing overdose deaths prolongs the average duration of opioid use, expanding the pool of active users and amplifying contact-driven initiation. This feedback can increase steady-state prevalence and ultimately raise total overdose mortality, even if individual lethality declines. When the life-saving benefit of naloxone is modest relative to this contagion effect (i.e., when $\delta_\ell$ exceeds $\bar{\delta}$), limited accessibility becomes preferable. Moreover, because $\bar{\delta}$ decreases as $\chi$ increases, higher baseline overdose rates can shift the system from a regime favoring full access (Case 1b) to one where restricting access (Case 2a) minimizes overall mortality. This framework thus provides policymakers with a quantitative basis for identifying when broader accessibility may inadvertently worsen epidemic outcomes.

At least for now, naloxone remains highly effective in reversing opioid overdoses, with a success rate ranging from 75% to 100% (Rzasa and Galinkin 2018). This high efficacy implies that $\delta_\ell$ is typically small, making it unlikely to exceed $\bar{\delta}$. Nevertheless, the growing prevalence of carfentanil—an opioid estimated to be 100 times more potent than fentanyl—raises serious concerns (New York Post 2024). Naloxone may be less effective in reversing overdoses involving such high-potency substances, which would increase $\delta_\ell$ and thereby make Case 2a more relevant. This concern is reinforced by emerging evidence suggesting that even high-dose naloxone formulations are not necessarily more effective in these scenarios (STAT 2024). Consequently, if carfentanil or similarly potent opioids become more widespread, the assumptions underlying the current optimal policy may no longer hold, and naloxone distribution and usage guidelines would need to be carefully reexamined. We revisit this issue in Section 7 through a calibrated analysis of future epidemic scenarios.

When $\beta > \bar{\beta}$ and $\delta_\ell < \bar{\delta} < \delta_h$, determining the optimal level of accessibility becomes more intricate. This complexity arises because, in Cases 1c and 2b, overdose mortality exhibits a non-monotonic relationship with accessibility, whereas in Cases 1a, 1b, and 2a, the relationship remains monotonic—either consistently decreasing or increasing. In the non-monotonic cases, mortality follows an inverted U-shaped pattern: moderate increases in accessibility may initially worsen outcomes before further expansion reduces mortality. This phenomenon, illustrated in Figure 3, highlights that incremental policy changes can sometimes be counterproductive. Accordingly, in such cases, identifying the optimal accessibility level requires direct comparison of the two extremes, $\theta = 0$ and $\theta = 1$, rather than relying on intermediate adjustments. This non-monotonicity has

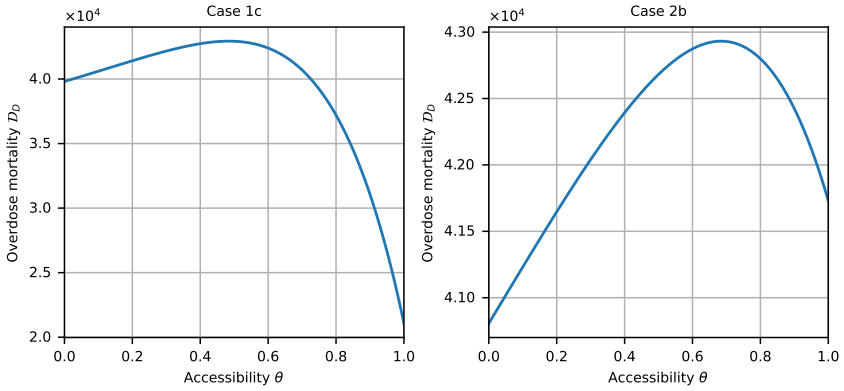


**Figure 3** **The impact of naloxone accessibility $\theta$ on overdose mortality. The specific parameter values used for each plot are provided in Table EC.4 in Appendix EC.5.**

important policy implications. Empirical findings by Packham (2022) show that modest expansions in syringe service programs promoting naloxone access may increase opioid-related deaths,

although this trend is not observed for more substantial expansions (Lambdin et al. 2023). While this result – often referred to as a *measurement problem* – has faced criticism in public health circles (New York Times 2024), our model suggests that such a counter-intuitive phenomenon is theoretically plausible. Modest increases in naloxone accessibility may fail to offset the increase in opioid misuse they trigger due to wider social interactions, potentially resulting in higher overdose mortality.

Next, Figure 4 illustrates the optimal naloxone accessibility policy $\theta^*$ under the D-SAS model across a range of OUD onset rates $\eta$ and transmission rates $\beta$. The figure partitions the $(\eta, \beta)$

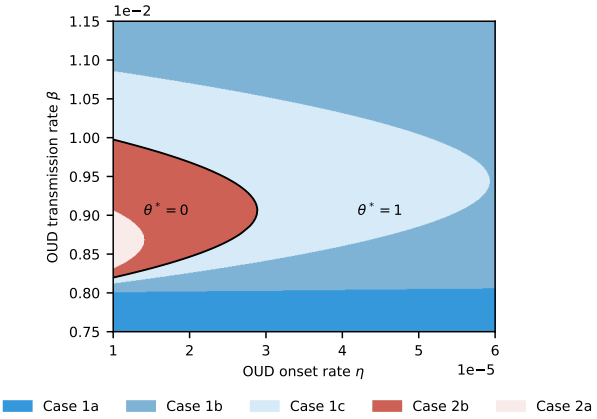


**Figure 4** **The optimal policy structure for the D-SAS model regarding $\beta$ and $\eta$ on the basis of D-SAS model. The parameters are $\Lambda = 2 \times 10^5$, $\gamma = 0.002$, $\alpha = 0.006$, $\delta_h = 0.75$, $\delta_\ell = 0.35$, $\chi = 0.002$.**

space into five distinct regions, each corresponding to a different case in Theorem 2. The region enclosed by the solid black line comprises two areas (Cases 2a and 2b), where zero accessibility is optimal. In contrast, the area outside the black line includes three regions (Cases 1a, 1b, and 1c), where full accessibility is optimal. In other words, holding other parameters fixed, full accessibility is optimal when either $\beta$ is relatively small or large, or when $\eta$ is relatively large. When $\beta$ is small, peer influence plays a limited role in opioid initiation, so increasing naloxone accessibility reduces mortality without triggering broader behavioral responses. When $\beta$ is large, social transmission may nonlinearly pull more susceptibles into the OUD group, enlarging the population exposed to overdose risk; hence, broadening naloxone accessibility is crucial to offset the corresponding rise in preventable deaths.

As for $\eta$, a high spontaneous initiation rate means that many individuals begin opioid use independently of social exposure. In such scenarios, the societal benefits of wide naloxone availability outweigh the risks, justifying full accessibility. Conversely, when $\beta$ is moderate and $\eta$ is low, opioid use remains relatively contained. In these cases, increasing accessibility has limited impact on reducing deaths, making zero accessibility the optimal policy.

## 6. Accounting for Moral Hazard in D-SAS-M Model

We now incorporate moral hazard into the D-SAS model, yielding the D-SAS-M model, illustrated in the bottom-right panel of Figure 1. This model is governed by the following system of differential equations:

$$\begin{cases} \dot{S}(t) = \Lambda - (\alpha+\eta)\, S(t) - \beta \dfrac{S(t)A(t)}{N(t)} + \gamma A(t), \\ \dot{A}(t) = \eta S(t) + \beta \dfrac{S(t)A(t)}{N(t)} - (\alpha + \gamma + (\chi+\Delta)\theta\delta_\ell + \chi(1-\theta)\delta_h)\, A(t), \\ N(t) = S(t) + A(t),\ \ S(t), A(t) \geq 0. \end{cases}$$

### 6.1. Optimization and Analysis

We denote the equilibrium of the D-SAS-M model by $(S^*_{D,M}, A^*_{D,M})$. Due to the complexity of the expressions, their closed-form representations are provided in Appendix EC.2.

The corresponding optimization problem that minimizes the long-run average overdose mortality is given by:

$$\begin{aligned} \min_{\theta\in[0,1]} \quad \mathcal{D}_{D,M}(\theta) &:= \lim_{T\to\infty} \frac{1}{T} \int_0^T \left((\chi+\Delta)\theta\delta_\ell + \chi(1-\theta)\delta_h\right) A(t)\, \mathrm{d}t \\ &= ((\chi+\Delta)\theta\delta_\ell + \chi(1-\theta)\delta_h) A^*_{D,M}. \end{aligned} \tag{6}$$

We start by defining the following revised threshold:

$$\bar{\delta}_M := \frac{\left(\beta - \bar{\beta}\right)^2 + 4\beta\eta}{2(\chi+\Delta)\left(\beta - \bar{\beta}\right)}.$$

Note that $\bar{\delta} > \bar{\delta}_M > 0$ when $\beta > \bar{\beta}$ and $\Delta > 0$. The joint presence of social contagion and moral hazard makes the policy characterization in Theorem 3 inherently more complex: the consequences of expanding accessibility now reflect not only epidemic dynamics but also behavioral responses to risk mitigation.

THEOREM 3 **(Optimal accessibility for the D-SAS-M model)**. *For problem (6), the optimal naloxone accessibility policy is as follows:*

1. ***Full accessibility is optimal*** *if any of the conditions in Table 1 holds.*

**Table 1** **Conditions under which full accessibility ($\theta = 1$) is optimal**

| Case | $\Delta$ vs. $\bar{\Delta}$ | $\beta$ vs. $\bar{\beta}$ | $\bar{\delta}$, $\bar{\delta}_M$ | Additional Condition |
|---|---|---|---|---|
| *a.* | $\Delta < \bar{\Delta}$ | $\beta \leq \bar{\beta}$ | – | – |
| *b.* | $\Delta < \bar{\Delta}$ | $\beta > \bar{\beta}$ | $\delta_h \leq \bar{\delta}$ | – |
| *c.* | $\Delta > \bar{\Delta}$ | $\beta > \bar{\beta}$ | $\delta_h \geq \bar{\delta}$ | – |
| *d.* | $\Delta < \bar{\Delta}$ | $\beta > \bar{\beta}$ | $\delta_h > \bar{\delta}$, $\delta_\ell < \bar{\delta}_M$ | $\mathcal{D}_{D,M}(\theta=1) < \mathcal{D}_{D,M}(\theta=0)$ |
| *e.* | $\Delta > \bar{\Delta}$ | $\beta > \bar{\beta}$ | $\delta_h < \bar{\delta}$, $\delta_\ell > \bar{\delta}_M$ | $\mathcal{D}_{D,M}(\theta=1) < \mathcal{D}_{D,M}(\theta=0)$ |

2. ***No accessibility is optimal*** *if any of the conditions in Table 2 holds.*

**Table 2 Conditions under which zero accessibility ($\theta = 0$) is optimal**

| Case | $\Delta$ vs. $\bar{\Delta}$ | $\beta$ vs. $\bar{\beta}$ | $\bar{\delta}$, $\bar{\delta}_M$ | Additional Condition |
|---|---|---|---|---|
| *a.* | $\Delta \geq \bar{\Delta}$ | $\beta \leq \bar{\beta}$ | – | – |
| *b.* | $\Delta \leq \bar{\Delta}$ | $\beta > \bar{\beta}$ | $\delta_\ell \geq \bar{\delta}_M$ | – |
| *c.* | $\Delta \geq \bar{\Delta}$ | $\beta > \bar{\beta}$ | $\delta_\ell \leq \bar{\delta}_M$ | – |
| *d.* | $\Delta \leq \bar{\Delta}$ | $\beta > \bar{\beta}$ | $\delta_h > \bar{\delta}$, $\delta_\ell < \bar{\delta}_M$ | $\mathcal{D}_{D,M}(\theta = 0) \leq \mathcal{D}_{D,M}(\theta = 1)$ |
| *e.* | $\Delta \geq \bar{\Delta}$ | $\beta > \bar{\beta}$ | $\delta_h < \bar{\delta}$, $\delta_\ell > \bar{\delta}_M$ | $\mathcal{D}_{D,M}(\theta = 0) \leq \mathcal{D}_{D,M}(\theta = 1)$ |

## 6.2. Interpreting Theorem 3: Policy Regimes and Decision Maps (with SAS-M Comparison)

According to Theorem 3, Figure 5 illustrates how the optimal naloxone accessibility policy depends on the overdose mortality rates $\delta_\ell$ and $\delta_h$, which represent mortality with and without naloxone, respectively. The blank area in the figure marks an infeasible region where $\delta_\ell \geq \delta_h$.

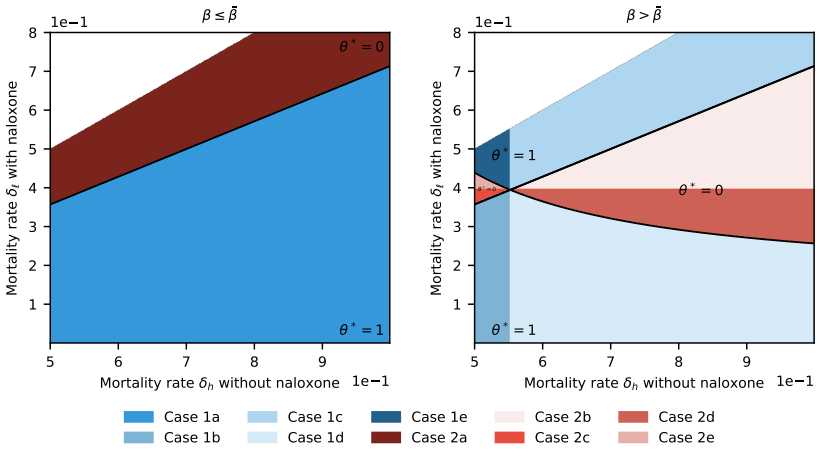


**Figure 5 The impact of mortality rate $\delta_\ell$ and $\delta_h$ on the optimal accessibility $\theta^*$ on the basis of D-SAS-M model. $\Delta = 0.005$ and $\chi = 0.0125$ for both plots. Other specific parameter values used for each plot are provided in Table EC.5 in Appendix EC.5.**

The effectiveness of naloxone increases with the gap $(\delta_h - \delta_\ell)$: smaller $\delta_\ell$ indicates stronger life-saving potential, making full accessibility more likely to be optimal in both panels of Figure 5. The black upward-sloping lines identify $(\delta_h, \delta_\ell)$ pairs for which the neutral effect threshold $\bar{\Delta}$ equals the degree of moral hazard $\Delta$. Combinations below the line correspond to $\bar{\Delta} > \Delta$, where naloxone's benefits dominate; those above the line indicate $\bar{\Delta} < \Delta$, where moral hazard outweighs its advantages.

The left panel represents epidemics primarily driven by prescription-induced addiction (i.e., $\beta \leq \bar{\beta}$). Here, the policy is determined solely by the comparison between $\bar{\Delta}$ and $\Delta$: full accessibility is optimal when $\bar{\Delta} > \Delta$, and zero accessibility when $\bar{\Delta} < \Delta$.

In contrast, the right panel captures contagion-dominant settings ($\beta > \bar{\beta}$), where social interactions amplify epidemic dynamics. The policy structure becomes richer and may even reverse relative to the left panel, as accessibility now affects both mortality and transmission. In particular, Cases 1c and 1e show that full accessibility can remain optimal even when $\Delta > \bar{\Delta}$. In such high-lethality environments, widespread naloxone access reduces overall exposure by accelerating the removal of individuals with OUD, thereby mitigating contagion effects. This mechanism echoes the classical *virulence–transmissibility trade-off* (Kun et al. 2023), in which higher lethality can limit overall spread. Nevertheless, moral hazard remains a serious individual-level concern, and our case study in Section 7 indicates that these extreme cases are unlikely under current epidemic conditions. However, as synthetic opioids become increasingly potent, such scenarios may grow more relevant, warranting proactive policy review.

Conversely, Cases 2b and 2d demonstrate that zero accessibility may be optimal even when naloxone provides individual benefits. In these cases, the relative advantage of naloxone's effectiveness over the mortality rate without it is marginal (that is, $(\delta_h - \delta_\ell)$ is relatively small). Given the intensified transmission risk and the potential for moral hazard in these circumstances, the optimal policy may be to completely restrict naloxone accessibility.

Figure 6 illustrates the optimal naloxone policy under the D-SAS-M model as a function of the transmission rate $\beta$ and the onset rate $\eta$. The left plot reflects cases where moral hazard $\Delta$ does not exceed the neutral threshold $\bar{\Delta}$, while the right plot shows the opposite. Each plot includes five distinct policy regions. When moral hazard is small (left panel), the optimal policy resembles

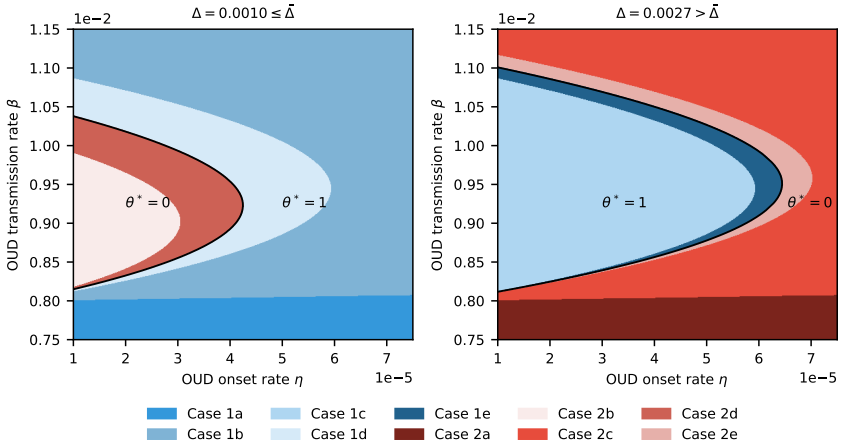


**Figure 6** **The optimal policy structure regarding $\beta$ and $\eta$ on the basis of D-SAS-M model. The parameters for both plots are $\Lambda = 2 \times 10^5$, $\gamma = 0.002$, $\alpha = 0.006$, $\delta_h = 0.75$, $\delta_\ell = 0.35$, $\chi = 0.002$, $\bar{\Delta} = 0.0023$.**

the structure of the D-SAS model in Figure 4. However, when moral hazard is substantial (right

panel), the policy structure reverses: optimal accessibility is 1 inside the region enclosed by the solid black curve and 0 outside.

As shown in the right plot, when both $\beta$ and $\eta$ are high, optimal accessibility drops to zero. In this case, elevated social transmission or onset rates increase overdose risk, and expanding naloxone access amplifies moral hazard, worsening the crisis. Full accessibility remains optimal only when $\beta$ is moderate and $\eta$ is low. Under these conditions, both social transmission and prescription-induced opioid use remain contained, and the negative consequences brought by moral hazard do not escalate significantly.

Under Cases d and e in Tables 1 and 2, the D-SAS-M model exhibits a unique inverted U-shaped relationship between accessibility $\theta$ and overdose mortality $\mathcal{D}_{D,M}$, as shown in Figure 7. This pattern, preserved by the D-SAS-M model, further supports the empirical findings of Packham (2022) under certain parameter configurations.

Figure 7 also reveals a counterintuitive outcome: stronger moral hazard does not always increase overdose deaths when social contagion is present. Holding accessibility constant at $\theta = 0.4$ (left) and $\theta = 0.6$ (right), higher moral hazard is associated with lower overdose mortality. Although this result may seem surprising from a policy perspective, the model suggests that in some cases, moral hazard could indirectly reduce long-term mortality by limiting the spread of OUD. An explicit analysis of this phenomenon is provided in Appendix EC.3.

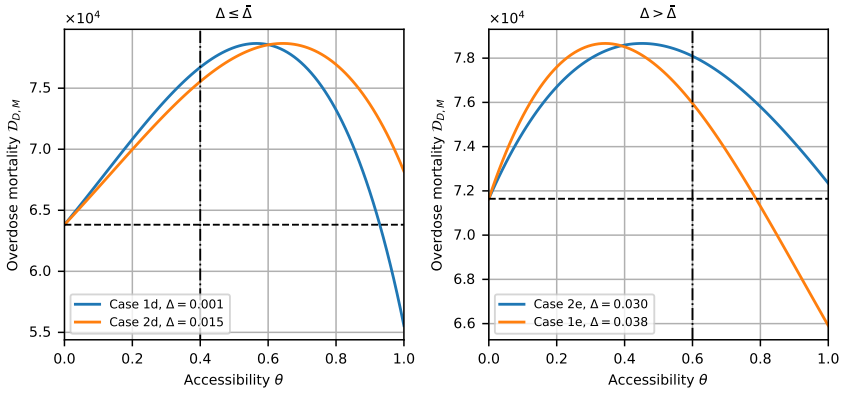


**Figure 7** **The impact of naloxone accessibility $\theta$ on overdose mortality on the basis of D-SAS-M model. For each plot, except for the moral hazard level, the other parameters remain the same, as detailed in Table EC.6 in Appendix EC.5.**

## 7. Case Study

To demonstrate the optimal accessibility policy and its real-world applicability, we conduct a case study based on data from the U.S. between 2010 and 2019. We begin with the calibration of

model parameters, followed by the presentation of key findings and a sensitivity analysis. The section concludes with a prospective analysis exploring the potential emergence of next-generation ultra-potent synthetic opioids.

### 7.1. Calibration of Model Parameters

Our SAS family of models focuses on the U.S. population aged 12 years and older to ensure consistency in the data scope used for parameter calibration. Table 3 first provides a summary of the estimated parameters in our models.

**Table 3 Summary of Estimations.**

| | Value | Unit | | Value | Unit | | Value | Unit | | Value | Unit |
|---|---|---|---|---|---|---|---|---|---|---|---|
| $\eta$ | 0.001116 | 1/year | $\Delta$ ((D)-SAS-M) | 0.000586 | 1/year | $\gamma$ | 0.022 | 1/year | $\Lambda$ | 4,142,545 | person/year |
| $\alpha$ | 0.009627 | 1/year | $\chi$ ((D)-SAS) | 0.003908 | 1/year | $\beta$ | 0.075914 | 1/year | $\delta_\ell$ | 0.125 | - |
| $\delta_h$ | 0.8925 | - | $\chi$ ((D)-SAS-M) | 0.003904 | 1/year | $\theta$ | 0.05 | - | | | |

We now describe the estimation details of each parameter. We begin by calibrating the model based on demographic and opioid-related data from the U.S. To estimate the natural death rate $\alpha$, we employ U.S. population data, total mortality data, and opioid overdose deaths, each disaggregated by year and age, obtained from the CDC WONDER database (2010–2019). We describe the procedure for retrieving these data from CDC WONDER database in Appendix EC.4.1. We then filter and aggregate these three datasets (population, total mortality, and overdose deaths) to generate annual time series restricted to individuals aged 12 years and older. We subtract opioid-related deaths from total deaths to isolate mortality from all other causes and estimate $\alpha$ via regression (see Appendix EC.4.2), obtaining $\alpha = 0.009627$. In addition, the average annual population of 12-year-old individuals over 2010–2019 is calculated and used as our estimate of the entry rate, $\Lambda = 4,142,545$ persons per year (see Appendix EC.4.2).

We next calibrate the opioid-specific parameters. Based on Rzasa and Galinkin (2018), naloxone successfully reverses 75% – 100% of overdoses. We conservatively set $\delta_\ell = 1 - \frac{0.75+1}{2} = 0.125$. For individuals without access to naloxone, overdose survival depends on emergency medical services (EMS). Ornato et al. (2020) report that the risk of death increases by 10% for every minute of delayed resuscitation. Survey data from Jakubowski et al. (2018) indicate that 43% of respondents had witnessed at least one overdose, and we optimistically assume all witnesses call EMS. Given typical EMS response times of 7 – 8 minutes (Johnson et al. 2021), we approximate the death rate without naloxone as: $\delta_h = (1 - 0.43) + 0.43 \times \frac{0.7+0.8}{2} = 0.8925$.

For the recovery rate $\gamma$, Luo and Stellato (2024) set the recovery rate at 0.1 for individuals receiving treatment for OUD. However, only approximately 22% of individuals with OUD receive

such treatment National Institute on Drug Abuse 2023, Jones et al. 2023). Accordingly, we approximate the overall recovery rate as: $\gamma = 0.1 \times 0.22 = 0.022$. For the OUD onset rate $\eta$, Battista et al. (2019) assume an annual opioid prescription rate of 0.15 per person and an OUD induction rate of 0.00744 among those prescribed. Thus, $\eta = 0.15 \times 0.00744 = 0.001116$.

To estimate the overdose rate $\chi$, we first approximate the overall opioid-related mortality rate, which is expressed as $\chi(\delta_h(1-\theta)+\delta_\ell\theta)$ in both the SAS and D-SAS models, and as $\chi(\delta_h(1-\theta)+\delta_\ell\theta)+\Delta\theta\delta_\ell$ in the SAS-M and D-SAS-M models. To this end, we use time series data on the U.S. OUD population aged 12 and over from 2010 to 2019 provided by Keyes et al. (2022), combined with opioid-related mortality data. Based on these datasets, we construct a regression model to estimate the total opioid-related mortality rate, which is found to be 0.003338 (see Appendix EC.4.2 for details). That is,

$$\chi(\delta_h(1-\theta)+\delta_\ell\theta) = 0.003338 \tag{7}$$

in the SAS and D-SAS models or

$$\chi(\delta_h(1-\theta)+\delta_\ell\theta)+\Delta\theta\delta_\ell = 0.003338 \tag{8}$$

in the SAS-M and D-SAS-M models.

For calibration purposes (i.e., to discipline other parameters before optimizing policy), we set a baseline access level $\theta^{\text{cal}}$ using observed bystander administration as a proxy for public-channel accessibility. Ornato et al. (2020) report that fewer than 5% of witnessed overdoses in the U.S. involved naloxone administration prior to 2020; we therefore take $\theta^{\text{cal}} \approx 0.05$ as a conservative baseline. This maps administration to our definition of $\theta$ (the share of individuals with OUD who have naloxone available at the time of an overdose) by treating administration as a lower bound on possession. Substituting this value into (7), we obtain $\chi = 0.003338 \times [0.05 \times 0.125 + 0.8925 \times 0.95]^{-1} = 0.003908$, which applies to both SAS and D-SAS models. This corresponds to approximately 3,908 overdose events per year per one million individuals with OUD.

Estimating the moral hazard parameter $\Delta$ is particularly challenging (when moral hazard exists), as behavioral responses to naloxone access are not directly observable. However, empirical studies offer useful proxies. Difference-in-differences and other quasi-experimental designs exploit variation in naloxone access laws to assess their effects on opioid-related outcomes (Abouk et al. 2019, Doleac and Mukherjee 2022, Packham 2022). We use the well-documented increase in opioid-related emergency department (ED) visits following the implementation of naloxone access laws as a proxy for moral hazard. Both Abouk et al. (2019) and Doleac and Mukherjee (2022) report an approximately 15% rise in opioid-related ED visits after the adoption of such laws. This increase is plausibly linked to a higher incidence of overdoses resulting from the moral hazard associated with broader naloxone

availability. Moreover, because the CDC (2024) recommends that patients with OUD who receive naloxone should still be transferred to the ED, the rise in ED visits could reasonably be interpreted as reflecting overdose attributable to this moral hazard. We therefore regard the increase in opioid-related ED visits as a reasonable proxy for assessing the extent of moral hazard. Formally, we set $\Delta = 0.15\chi$ in the baseline and examine wider ranges in robustness checks in Section 7.2. Substituting this relation into (8) yields $\chi = 0.003338 \times [0.05 \times 0.125 + 0.8925 \times 0.95 + 0.15 \times 0.05 \times 0.125]^{-1} = 0.003904$, and hence $\Delta = 0.000586$ in the SAS-M and D-SAS-M models. This indicates that in the OUD population without naloxone access, there are on average about 3,904 overdose events per one million individuals per year. In contrast, among those with access to naloxone, the annual number of overdose events is approximately 586 higher per one million individuals, reflecting the behavioral increase associated with moral hazard. Notice that we do not use the mortality data reported in Abouk et al. (2019) and Doleac and Mukherjee (2022) to estimate the level of moral hazard, since their measure is standardized per 100,000 of the general population, whereas in our models, the mortality rate is restricted to the OUD population.

Finally, we estimate the transmission rate $\beta$ in the D-SAS-M model using a regression-based approach, yielding $\beta = 0.075914$ (see Appendix EC.4.2 for details). This implies that, on average, each person in the U.S. has approximately 0.075914 effective contacts per year that could result in the transmission of OUD (Hethcote 2000). The next section presents the case study findings and assesses the robustness of the results through sensitivity analysis.

### 7.2. Case Study Findings

We now present the representative cases for each model, derived from the calibrated parameter estimates. As summarized in Table 4, full accessibility consistently emerges as the optimal policy across all models. This finding reinforces the FDA's recommendation to expand naloxone access as a central strategy for reducing overdose mortality in the context of the opioid crisis.

**Table 4 Representative cases for each model using calibrated parameters.**

| Model | $\bar{\Delta} - \Delta$ | $\beta - \bar{\beta}$ | $\bar{\delta}$ | $\bar{\delta}_M$ | Corresponding case | $\theta^*$ |
|---|---|---|---|---|---|---|
| SAS | – | – | – | – | – | 1 |
| SAS-M | 0.023384 | – | – | – | – | 1 |
| D-SAS | – | 0.043171 | 6.527727 | – | Case 1b in Theorem 2 | 1 |
| D-SAS-M | 0.023384 | 0.043171 | 6.534415 | 5.681594 | Case 1b in Theorem 3 | 1 |

Moreover, the observed difference $\bar{\Delta} - \Delta$ suggests that the moral hazard effect remains relatively mild. This indicates that, at present, naloxone's high efficacy in reversing opioid-induced respiratory depression continues to outweigh potential compensatory increases in opioid misuse, supporting its

role as an effective harm reduction measure. In addition, we observe that $\beta - \bar{\beta} > 0$, which indicate that incorporating social transmission mechanisms into epidemic models could help capture certain aspects of the dynamics of opioid addiction.

***Sensitivity Analyses.*** We also examine how varying levels of moral hazard and overdose rate influence the optimal naloxone accessibility policy in the SAS-M and D-SAS-M models. The estimates of the overdose rate $\chi$ and moral hazard $\Delta$ are jointly constrained to satisfy $\chi\left(\delta_h(1-\theta)+\delta_\ell\theta\right)+\Delta\theta\delta_\ell = 0.003338$. As the overdose rate increases, the estimated moral hazard decreases, leading to a lower $\Delta/\chi$ ratio and a higher neutral-effect threshold. Naloxone's life-saving effectiveness is meaningfully compromised only when $\Delta/\chi$ exceeds 6.14, corresponding to an overdose rate below 0.003740, at which point the optimal policy shifts to zero accessibility in both models. While no clear empirical evidence currently suggests that moral hazard reaches such extreme levels, this possibility cannot be entirely excluded, though under present real-world conditions, full naloxone accessibility likely remains the optimal policy.

### 7.3. Prospective Analysis: The Potential Emergence of Next-generation Ultra-potent Synthetic Opioids

We recognize that the continuous evolution of illicit opioids has resulted in increasingly potent and hazardous substances. As highlighted by the concern expressed in Section 5.1, the progression from traditional morphine to OxyContin (approximately 1.5 times more potent and widely regarded as a catalyst of the U.S. opioid crisis), followed by heroin (roughly twice as potent), and now fentanyl (50–100 times more potent), illustrates a clear pattern: each significant increase in potency has triggered a new wave of the epidemic, heightening overdose risks and intensifying public health challenges.

In this section, we further examine whether the FDA should proactively reassess its current policy of expanding naloxone accessibility, particularly in anticipation of future scenarios where the crisis may be driven by even more potent synthetic opioids—such as carfentanil (approximately 10,000 times stronger than morphine), ohmefentanyl (averaging 6,300 times more potent, with one isomer reaching up to 18,000 times (Yong et al. 2003)), or other similarly powerful analogs. These substances may substantially increase the overdose rate $\chi$ and reduce naloxone's effectiveness, as reflected by higher $\delta_\ell$. Additionally, these substances can increase overdose risk by complicating withdrawal and acute management and by accelerating tolerance, which drives dose escalation. Clinical guidance and recent studies in the fentanyl era document more complex withdrawal presentations and induction challenges (Weimer et al. 2023, Thakrar et al. 2024), and national guidance notes that higher opioid dosages are associated with increased overdose risk (CDC 2022, SAMHSA 2025). Evidence on naloxone's effectiveness against carfentanil is still limited and mixed; animal

studies report incomplete reversal and prolonged toxicity in some settings despite naloxone administration (Langston et al. 2020).

Assuming no moral hazard, we retain the parameter estimates from Section 7.1 and focus on how changes in $\chi$ and $\delta_\ell$ influence the optimal policy. In the basic SAS model, it is well established that as long as naloxone provides even a slight therapeutic benefit, full accessibility remains the optimal policy. However, the dynamics shift in the D-SAS model. As illustrated in Figure 8, the emergence of more potent and harmful opioids significantly alters the policy landscape. Notably, when both the overdose rate and the likelihood of severe withdrawal or increased use are high, the optimal policy shifts to zero accessibility (upper-right region of Figure 8) for FDA. For instance, if a potent opioid elevates the overdose rate $\chi$ to nine times its original value and raises $\delta_\ell$ to 0.7 (black dot in Figure 8), the optimal level of accessibility drops to zero. Although we cannot definitively claim that the upper-right region of Figure 8 precisely reflects future scenarios, it is important to recognize that fentanyl already presents extreme risks, and the potency of carfentanil and ohmefentanyl far exceeds that of fentanyl. We therefore recommend that the FDA carefully reassess naloxone accessibility policies should these more dangerous opioids continue to proliferate.

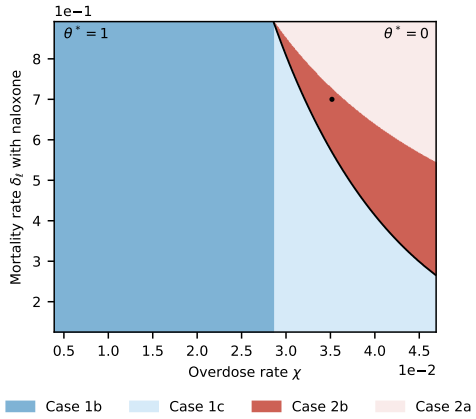


**Figure 8** **Optimal naloxone accessibility under increasingly potent opioids in the D-SAS model. Cases correspond to those in Theorem 2, with parameters calibrated as in Section 7.1.**

When moral hazard is taken into account, the influence of more potent opioids on optimal policy becomes more nuanced. It is not immediately clear whether such substances would raise or lower the neutral effect threshold, as this depends on the relative changes in the overdose rate $\chi$ and the mortality rate under naloxone treatment $\delta_\ell$. In addition, notice that more potent opioids may exacerbate moral hazard by increasing physiological dependence and reinforcing risky use patterns. But, in the SAS-M model without interaction terms, the optimal naloxone accessibility

level remains at 1, provided that the moral hazard level stays below the neutral effect threshold associated with these stronger substances.

In contrast, for the D-SAS-M model, the optimal accessibility may be completely different. Figure 9 illustrates how the combination of more potent opioids and moral hazard affects accessibility decisions. For both plots, the lower regions of the upward-sloping black curve represent scenarios where the neutral effect threshold exceeds the level of moral hazard, while the upper regions correspond to cases where the moral hazard level surpasses the threshold. Note that, if more potent opioids substantially reduce the effectiveness of naloxone in reversing overdoses, without causing a corresponding significant increase in the overdose rate (represented by the upper-left regions in both plots of Figure 9), the optimal policy shifts to zero accessibility. In such cases, expanding naloxone access may backfire, increasing overdose incidents under conditions of low survival likelihood.

Interestingly, when a highly potent and easily transmissible synthetic opioid results in both a significantly elevated overdose rate $\chi$ and a higher mortality rate even with naloxone administration $\delta_\ell$ (corresponding to the upper-right regions in both plots of Figure 9), the optimal policy for the FDA remains full naloxone accessibility ($\theta^* = 1$). This finding differs from the result observed in the D-SAS model, where full accessibility is not always optimal. This is because, in the upper-right regions where moral hazard exceeds the threshold $\bar{\Delta}$, greater naloxone accessibility may coincide with higher overall mortality in the OUD population, while reducing the exposure risk for susceptible groups in a socially driven opioid crisis. Therefore, full accessibility emerges as the optimal policy. Furthermore, we observe that as the level of moral hazard increases, the upper-right and upper-left regions expand, indicating that moral hazard has an increasingly pronounced effect on the structure of the optimal policy.

These findings together suggest that, in the presence of significant moral hazard and more lethal synthetic opioids, the FDA may need to revisit and reassess naloxone accessibility policies with heightened caution.

## 8. Conclusions and Future Directions

This paper examines a central public health question: how expanded naloxone accessibility affects the opioid epidemic, particularly overdose mortality. While some studies suggest that broader access may worsen outcomes through moral hazard, others highlight its life-saving role. To reconcile these perspectives, we develop an analytical framework that identifies optimal naloxone accessibility policies under varying epidemic conditions.

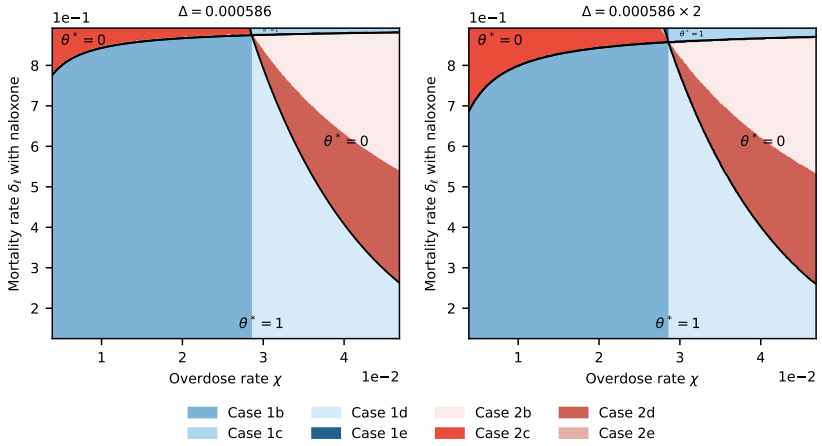


**Figure 9** **Optimal naloxone accessibility under increasingly potent opioids in the D-SAS-M model. Cases correspond to those in Theorem 3, with parameters given in Section 7.1.**

*Summary of Optimal Naloxone Accessibility Across Models.* We propose four progressively richer models that capture the key epidemiological and behavioral mechanisms of the opioid crisis and characterize how the structure of the optimal accessibility policy evolves:

- **SAS Model (Baseline):** Without moral hazard or social contagion, full accessibility is always optimal.
- **SAS-M Model (Incorporating Moral Hazard):** Introducing moral hazard yields a bang-bang policy. Full accessibility is optimal when the behavioral response to naloxone ($\Delta$) remains below a critical threshold; otherwise, restricted access is preferable.
- **D-SAS Model (Adding Social Contagion):** Peer-driven opioid misuse introduces additional complexity. Full accessibility remains optimal when transmission rates are low or naloxone is highly effective, but limited accessibility can better mitigate mortality under certain conditions.
- **D-SAS-M Model (Moral Hazard and Social Contagion Combined):** The most comprehensive model retains the bang-bang structure, with optimal accessibility determined by the interaction between moral hazard, contagion dynamics, and naloxone effectiveness. Detailed conditions are summarized in Tables 1 and 2.

*Policy Implications.* Our analysis offers structured guidance for designing naloxone distribution policies that balance life-saving benefits against behavioral risks. The policy thresholds derived from our models link empirical estimates of naloxone effectiveness and behavioral response to recommended access levels, providing policymakers with a transparent and adaptable decision-support tool.

While full accessibility is often optimal—particularly in prescription-driven epidemics—emerging dynamics such as social contagion or the rise of ultra-potent opioids like carfentanil may shift this

conclusion. The relationship between accessibility and overdose mortality can be non-monotonic, with moderate expansions initially worsening outcomes before improving them at higher access levels.

A calibrated U.S. case study illustrates the framework's practical relevance: under current conditions, full accessibility remains optimal, aligning with existing regulatory policy. However, this result depends on epidemic parameters, which may evolve with changing potency or transmission intensity, necessitating ongoing policy reassessment.

*Bang–bang accessibility.* Our results show a *bang–bang policy*, that is, the optimal naloxone accessibility lies at one of the two extremes—either full or none—rather than at an intermediate level. This structure emerges in our models because accessibility simultaneously affects both life-saving and risk-inducing mechanisms, creating opposing forces that lead the optimal policy to settle at an endpoint under the modeled assumptions. A binary recommendation is operationally useful in health policy: it is simple to communicate, implement, and audit, and it matches the yes/no nature of core access levers (e.g., OTC status, statewide standing orders, publicly funded distribution). In practice, sustaining "partial" access (such as quotas or loosely targeted dispensing) is harder to administer at scale and prone to drift.

However, bang–bang outcomes also have limitations. While the structure is robust across a broad range of parameters, boundary cases—where the system lies near the switching threshold between full and zero accessibility—require careful and accurate estimation of key parameters, such as behavioral responses or naloxone effectiveness. In these situations, small changes in the underlying conditions could shift the optimal recommendation, underscoring the importance of precise empirical calibration and continuous monitoring as epidemic dynamics evolve.

Recall that even when the model recommends limited public accessibility ($\theta = 0$), naloxone remains available through medical channels, ensuring clinical use under professional judgment. Real-world policies must therefore integrate naloxone access with complementary interventions—such as prevention, treatment expansion, and controlled prescribing—to address the crisis holistically.

*Future Research Directions.* Several extensions can further enhance the policy relevance and realism of our framework. First, while our analysis focuses on steady-state outcomes, policymakers often face short-term versus long-term trade-offs. For instance, during overdose surges, reducing immediate mortality may take precedence even if riskier behaviors raise future prevalence. Extending the model to finite-horizon or time-varying policies would allow optimization of cumulative deaths over the next several months under practical constraints (budget, staffing, distribution capacity) and enable comparison with the steady-state recommendation. This lets us test rules that switch to expanded naloxone access when overdoses surge, focus temporary increases on high-risk settings

(e.g., paramedic "leave-behind" naloxone kits or on-site distribution in shelters), and then taper back once indicators improve. A rolling-horizon optimization approach can re-optimize access as overdose rates, potency signals, or response times evolve, explicitly trading off short-run mortality reduction against longer-run prevention.

Second, cost-benefit analyses that integrate both epidemiological outcomes and operational realities are essential. For example, recent efforts to deploy naloxone vending machines in Oklahoma were curtailed due to high costs and logistical challenges (2 News Oklahoma 2024). Future work should incorporate such economic and operational factors to inform sustainable, context-specific naloxone policies.

Finally, the calibrated results in the case study suggest that social transmission mechanisms play a critical role in shaping the dynamics of the opioid epidemic. Our simplified models highlight these mechanisms and yield transparent, threshold-based policy rules. Building on this foundation, future research should integrate detailed social network data and empirical evidence to better capture interaction-driven dynamics, especially as the COVID-19 pandemic has amplified the role of social channels in opioid misuse.

## Acknowledgments

The authors sincerely thank Editor Sergei Savin, the anonymous Senior Editor and reviewers for their insightful and constructive feedback, which has greatly strengthened this work. Partial financial support was provided by the Israel Science Foundation [Grant 277/21] and the Bernard M. Gordon Center for Systems Engineering at the Technion.

## References

2 News Oklahoma. 2024. Oklahoma pulls plug on free narcan, fentanyl test strip vending machines. https://www.kjrh.com/news/local-news/oklahoma-pulls-plug-on-free-narcan-fentanyl-test-strip-vending-machines Retrieved November 23, 2025.

Abouk, R., R.L. Pacula, D. Powell. 2019. Association between state laws facilitating pharmacy distribution of naloxone and risk of fatal overdose. *JAMA Internal Medicine*, 179 (6), 805-811.

Abramson, A. 2021. Substance use during the pandemic. *Monitor on Psychology*, 52 (2), 22.

Adamopoulou, E., J. Greenwood, N. Guner, K. Kopecky. 2024. The role of friends in the opioid epidemic, (working paper).

Ansari, S., S. Enayati, R. Akhavan-Tabatabaei, J. Kapp. 2024. Curbing the opioid crisis: Optimal dynamic policies for preventive and mitigating interventions. *Decision Analysis*, 21 (3), 165-193.

Ardeljan, A.D., B. Fiedler, L. Fiedler, G.R. Luck, D.G. Maki, L. Clayton. 2023. Naloxone over the counter: Increasing opportunities and challenges for health providers. *The American Journal of Medicine*, 136 504-506.

Attari, I., J. Helm, J. Mejia. 2025. Hiding behind complexity: Supply chain, oversight, race, and the opioid crisis. *Production and Operations Management*, 34 (4), 725-743.

Battista, N., L. Pearcy, W. Strickland. 2019. Modeling the prescription opioid epidemic. *Bulletin of Mathematical Biology*, 81 2258-2289.

Baucum, M., M. Harris, L.e Kessler, G. Lu. 2025. Reducing overdose deaths and mitigating county disparities: Optimal allocation of substance use treatment centers. *Manufacturing & Service Operations Management*, 27 (3), 736-756.

Bertsimas, D., M. Fazel-Zarandi, J. Ivanhoe, P. Petridis. 2025. Early detection of opioid over-procurement: A semisupervised machine learning approach. *Manufacturing & Service Operations Management*, 27 (6), 1889-1904.

Bobroske, K., M. Freeman, L. Huan, A. Cattrell, S. Scholtes. 2022. Curbing the opioid epidemic at its root: The effect of provider discordance after opioid initiation. *Management Science*, 68 (3), 2003-2015.

Burris, S., L. Beletsky, C. Castagna, C. Coyle, C. Crowe, J. McLaughlin. 2009. Stopping an invisible epidemic: Legal issues in the provision of naloxone to prevent opioid overdose. *Drexel Law Review*, 1 273.

Cawley, J., D. Dragone. 2024. Harm reduction for addictive consumption: When does it improve health and when does it backfire? *Journal of Health Economics*, 98 102931.

CDC. 2022. Cdc clinical practice guideline for prescribing opioids for pain — United States, 2022. https://www.cdc.gov/mmwr/volumes/71/rr/rr7103a1.htm Retrieved November 23, 2025.

CDC. 2024. 5 things to know about naloxone. https://www.cdc.gov/overdose-prevention/reversing-overdose/about-naloxone.html Retrieved November 23, 2025.

Chehrazi, N., L. E Cipriano, E. Enns. 2019. Dynamics of drug resistance: Optimal control of an infectious disease. *Operations Research*, 67 (3), 619-650.

CNN. 2017. Trump: 'the opioid crisis is an emergency'. https://edition.cnn.com/2017/08/10/health/trump-opioid-emergency-declaration-bn Retrieved November 23, 2025.

Cole, S., M.F. Olive, Wirkus S. 2024. The dynamics of heroin and illicit opioid use disorder, casual use, treatment, and recovery: A mathematical modeling analysis. *Mathematical Biosciences and Engineering*, 21 3165-3206.

Cole, S., S. Wirkus. 2022. Modeling the dynamics of heroin and illicit opioid use disorder, treatment, and recovery. *Bulletin of Mathematical Biology*, 84 (4), 48.

Djilali, S., T. Touaoula, Sofiane E. Miri. 2017. A heroin epidemic model: Very general non linear incidence, treat-age, and global stability. *Acta Applicandae Mathematicae*, 152 171-194.

Doleac, J., A. Mukherjee. 2022. The effects of naloxone access laws on opioid abuse, mortality, and crime. *The Journal of Law and Economics*, 65 (2), 211-238.

Drug Enforcement Administration. 2025. Controlled substances - alphabetical order. https://www.deadiversion.usdoj.gov/schedules/orangebook/c_cs_alpha.pdf Retrieved November 23, 2025.

Euractiv. 2024. Sweden makes naloxone spray an otc product, to prevent opioid overdose deaths. https://www.euractiv.com/section/health-consumers/news/sweden-makes-Naloxone-spray-an-otc-product-to-prevent-opioid-overdose-deaths/ Retrieved November 23, 2025.

Gan, K., Y. Tang, A. Scheller-Wolf, S. Tayur. 2025. Optimizing wearable devices in personalized opioid use disorder treatments under budget constraint, (working paper).

Gao, X., N. Kong, P. Griffin. 2024. Shortening emergency medical response time with joint operations of uncrewed aerial vehicles with ambulances. *Manufacturing & Service Operations Management*, 26 (2), 447-464.

Gökçınar, A., M. Çakanyıldırım, T. Price, M. Adams. 2022. Balanced opioid prescribing via a clinical trade-off: Pain relief vs. adverse effects of discomfort, dependence, and tolerance/hypersensitivity. *Decision Analysis*, 19 (4), 297-318.

Greene, J. 2018. Naloxone "moral hazard" debate pits economists against physicians. *Annals of Emergency Medicine*, 72 (2), A13-A16.

Haley, D.F., R. Saitz. 2020. The opioid epidemic during the COVID-19 pandemic. *JAMA*, 324 (16), 1615-1617.

Hardin, J., J. Seltzer, H. Galust, A. Deguzman, I. Campbell, N. Friedman, G. Wardi, R.F. Clark, D. Lasoff. 2024. Emergency department take-home naloxone improves access compared with pharmacy-dispensed naloxone. *The Journal of Emergency Medicine*, 66 (4), e457-e462.

Hethcote, H. 2000. The mathematics of infectious diseases. *SIAM Review*, 42 (4), 599-653.

Houser, R. 2023. Expanding access to naloxone: A necessary step to curb the opioid epidemic. *Disaster Medicine and Public Health Preparedness*, 17 e245.

Huang, G., A. Liu. 2013. A note on global stability for a heroin epidemic model with distributed delay. *Applied Mathematics Letters*, 26 (7), 687-691.

Jakubowski, A., H. Kunins, Z. Huxley-Reicher, A. Siegler. 2018. Knowledge of the 911 good samaritan law and 911-calling behavior of overdose witnesses. *Substance Abuse*, 39 (2), 233-238.

Jawa, R., S. Murray, M. Tori, J. Bratberg, A. Walley. 2022. Federal policymakers should urgently and greatly expand naloxone access. *American Journal of Public Health*, 112 (4), 558-561.

Johnson, A., C. Cunningham, E. Arnold, W. Rosamond, J. Zègre-Hemsey. 2021. Impact of using drones in emergency medicine: What does the future hold? *Open Access Emergency Medicine*, 13 487-498.

Jones, C., B. Han, G. Baldwin, E. Einstein, W. Compton. 2023. Use of medication for opioid use disorder among adults with past-year opioid use disorder in the US, 2021. *JAMA Network Open*, 6 (8), e2327488-e2327488.

KC, D., T. Kim, J. Liu. 2022. Electronic prescription monitoring and the opioid epidemic. *Production and Operations Management*, 31 (11), 4057-4074.

Keyes, K., C. Rutherford, A. Hamilton, J. Barocas, K. Gelberg, P. Mueller, D. Feaster, N. El-Bassel, M. Cerdá. 2022. What is the prevalence of and trend in opioid use disorder in the United States from 2010 to 2019? Using multiplier approaches to estimate prevalence for an unknown population size. *Drug and Alcohol Dependence Reports*, 3 100052.

Kun, Á., A. Hubai, A. Král, J. Mokos, B. Mikulecz, Á. Radványi. 2023. Do pathogens always evolve to be less virulent? The virulence–transmission trade-off in light of the COVID-19 pandemic. *Biologia Futura*, 74 (1), 69-80.

Lambdin, B., R. Bluthenthal, J. Humphrey, P. LaKosky, S. Prohaska, A. Kral. 2023. 'new evidence' for syringe services programs? A call for rigor and skepticism. *International Journal of Drug Policy*, 121 104107.

Langston, J., M. Moffett, J. Makar, B. Burgan, T. Myers. 2020. Carfentanil toxicity in the African green monkey: Therapeutic efficacy of naloxone. *Toxicology Letters*, 325 34-42.

Lejeune, M., W. Ma. 2025. Drone-delivery network for Opioid overdose: Nonlinear integer queueing-optimization models and methods. *Operations Research*, 73 (1), 86-108.

Li, M., H. Bouardi, O. Lami, T. Trikalinos, N. Trichakis, D. Bertsimas. 2023. Forecasting COVID-19 and analyzing the effect of government interventions. *Operations Research*, 71 (1), 184-201.

Liu, J., A. Bharadwaj. 2020. Drug abuse and the internet: Evidence from craigslist. *Management Science*, 66 (5), 2040-2049.

Liu, Y., K. Xie, W. Chen. 2025. Recreational cannabis legalization and illicit drugs: Drug usage, mortality, and darknet transactions. *Production and Operations Management*, 34 (1), 99-119.

Luo, J., B. Stellato. 2024. Frontiers in operations: Equitable data-driven facility location and resource allocation to fight the opioid epidemic. *Manufacturing & Service Operations Management*, 26 (4), 1229-1244.

Mars, S., P. Bourgois, G. Karandinos, F. Montero, D. Ciccarone. 2014. "Every 'never' I ever said came true": Transitions from opioid pills to heroin injecting. *International Journal of Drug Policy*, 25 (2), 257-266.

Martcheva, M. 2015. *An introduction to mathematical epidemiology*, vol. 61. Springer.

Mehrez, A., A. Gafni. 1987. The optimal treatment strategy—a patient's perspective. *Management Science*, 33 (12), 1602-1612.

Messinger, J., L. Beletsky, A. Kesselheim, R. Barenie. 2023. Moving naloxone over the counter is necessary but not sufficient. *Annals of Internal Medicine*, 176 (8), 1109-1112.

National Institute on Drug Abuse. 2023. Only 1 in 5 u.s. adults with opioid use disorder received medications to treat it in 2021. https://nida.nih.gov/news-events/news-releases/2023/08/only-1-in-5-us-adults-with-opioid-use-disorder-received-medications-to-treat-it-in-2021 Retrieved November 23, 2025.

National Institute on Drug Abuse. 2024. Overdose death rates. https://nida.nih.gov/research-topics/trends-statistics/overdose-death-rates Retrieved November 23, 2025.

New York Post. 2024. CDC warns of carfentanil, an opioid that's 100 times more potent than fentanyl. https://nypost.com/2024/12/10/us-news/cdc-warns-rise-in-opioid-thats-100-times-more-potent-than-fentanyl/ Retrieved November 23, 2025.

New York Times. 2024. Moral hazard has no place in addiction treatment. https://www.nytimes.com/2024/03/01/opinion/moral-hazard-drug-addiction.html Retrieved November 23, 2025.

Ornato, J., A. You, G. McDiarmid, L. Keyser-Marcus, A. Surrey, J. Humble, S. Dukkipati, L. Harkrader, S. Davis, J. Moyer, D. Tidwell, M. Peberdy. 2020. Feasibility of bystander-administered naloxone delivered by drone to opioid overdose victims. *The American Journal of Emergency Medicine*, 38 (9), 1787-1791.

Packham, A. 2022. Syringe exchange programs and harm reduction: New evidence in the wake of the opioid epidemic. *Journal of Public Economics*, 215 104733.

Peltzman, S. 1975. The effects of automobile safety regulation. *Journal of Political Economy*, 83 (4), 677-725.

Pernell, K., J. Jung. 2024. Rethinking moral hazard: Government protection and bank risk-taking. *Socio-Economic Review*, 22 (2), 625-653.

Qayyum, S., R. Ansari, I. Ullah, D. Siblini. 2023. The FDA approves the second OTC naloxone–a step toward opioid crisis mitigation. *International Journal of Surgery*, 109 (12), 4349.

Rao, I., K. Humphreys, M. Brandeau. 2021. Effectiveness of policies for addressing the US opioid epidemic: A model-based analysis from the Stanford-Lancet commission on the north American opioid crisis. *The Lancet Regional Health–Americas*, 3 100031.

Reider, B. 2019. Opioid epidemic. *The American Journal of Sports Medicine*, 47 (5), 1039-1042.

Rzasa, L., J. Galinkin. 2018. Naloxone dosage for opioid reversal: Current evidence and clinical implications. *Therapeutic Advances in Drug Safety*, 9 (1), 63-88.

Saberi, S., S. Moore, S. Li, R. Mather, M. Daniels, A. Shahani, A. Barreveld, T. Griswold, P. McGuire, H. Connery. 2024. Systemized approach to equipping medical students with naloxone: a student-driven initiative to combat the opioid crisis. *BMC Medical Education*, 24 (1), 241.

Sagberg, F., S. Fosser, I. Sætermo. 1997. An investigation of behavioural adaptation to airbags and antilock brakes among taxi drivers. *Accident Analysis & Prevention*, 29 (3), 293-302.

SAMHSA. 2025. Overdose prevention and response toolkit. https://library.samhsa.gov/sites/default/files/overdose-prevention-response-kit-pep23-03-00-001.pdf Retrieved November 23, 2025.

Seamans, M., T. Carey, D. Westreich, S. Cole, S. Wheeler, G. Alexander, V. Pate, M. Brookhart. 2018. Association of household opioid availability and prescription opioid initiation among household members. *JAMA Internal Medicine*, 178 (1), 102-109.

Spencer, N. 2023. Does drug decriminalization increase unintentional drug overdose deaths?: Early evidence from oregon measure 110. *Journal of Health Economics*, 91 102798.

STAT. 2024. Higher naloxone doses have no impact on overdose survival, study shows. https://www.statnews.com/2024/02/08/narcan-high-dose-naloxone-overdose/ Retrieved November 23, 2025.

Thakrar, A.P, P.J. Christine, A. Siaw-Asamoah, A. Spadaro, S. Faude, C.K. Snider, M.K. Delgado, M. Lowenstein, K. Kampman, J. Perrone. 2024. Buprenorphine-precipitated withdrawal among hospitalized patients using fentanyl. *JAMA Network Open*, 7 (9), e2435895-e2435895.

The Washington Post. 2018. The moral hazard of naloxone in the opioid crisis. https://www.washingtonpost.com/opinions/the-moral-hazard-of-naloxone-in-the-opioid-crisis/2018/03/08/c3584f16-2259-11e8-86f6-54bfff693d2b_story.html Retrieved November 23, 2025.

The Washington Post. 2023. Everyone should have narcan in their homes. https://www.washingtonpost.com/opinions/2023/03/29/narcan-over-the-counter-fda-approval/ Retrieved November 23, 2025.

Tse, W., F. Djordjevic, V. Borja, L. Picco, T. Lam, A. Olsen, S. Larney, P. Dietze, S. Nielsen. 2022. Does naloxone provision lead to increased substance use? A systematic review to assess if there is evidence of a 'moral hazard'associated with naloxone supply. *International Journal of Drug Policy*, 100 103513.

Weimer, M.B., A.A. Herring, S.S. Kawasaki, M. Meyer, B.A. Kleykamp, K.S. Ramsey. 2023. Asam clinical considerations: buprenorphine treatment of opioid use disorder for individuals using high-potency synthetic opioids. *Journal of Addiction Medicine*, 17 (6), 632-639.

World Health Organization. 2024. Opioid overdose. https://www.who.int/news-room/fact-sheets/detail/opioid-overdose Retrieved November 23, 2025.

Yang, J., A. Mishra. 2025. Diversion in prescription opioid supply chains: Evidence from the drug supply chain security act. *Manufacturing & Service Operations Management*, 27 (3), 679-699.

Yong, Z., W. Hao, Y. Weifang, D. Qiyuan, C. Xinjian, J. Wenqiao, Z. Youcheng. 2003. Synthesis and analgesic activity of stereoisomers of cis-fluoro-ohmefentanyl. *Die Pharmazie-An International Journal of Pharmaceutical Sciences*, 58 (5), 300-302.

Zaric, G., M. Brandeau, P. Barnett. 2000. Methadone maintenance and HIV prevention: A cost-effectiveness analysis. *Management Science*, 46 (8), 1013-1031.

Zhou, J., J. Cai, Athanasios A. Pantelous, Z. Li, M. Li. 2025. A decision-making framework for supporting an equitable global vaccine distribution under humanitarian perspectives. *European Journal of Operational Research*, 327 (2), 655-672.

# E-Companion: *Expanding Naloxone Accessibility: A Lifesaver or a Risky Setback?*

## EC.1. Analysis of the D-SAS Model with Mass-Action Incidence $\beta S(t)A(t)$

The dynamics of the D-SAS model under mass action incidence, represented by the term $\beta S(t)A(t)$, are governed by the following system of differential equations:

$$\begin{cases} \dot{S}(t) = \Lambda - (\alpha+\eta)S(t) - \beta S(t)A(t) + \gamma A(t), \\ \dot{A}(t) = \eta S(t) + \beta S(t)A(t) - \chi\theta\delta_\ell A(t) - \chi(1-\theta)\delta_h A(t) - \alpha A(t) - \gamma A(t), \\ S(t) \geq 0, \quad A(t) \geq 0. \end{cases} \tag{EC.1.1}$$

Let $\rho = \alpha(\alpha+\gamma+\eta) - \beta\Lambda + \chi(\alpha+\eta)\left(\theta\delta_\ell + (1-\theta)\delta_h\right)$. The only feasible equilibrium point of system (EC.1.1) is given by:

$$(S_D^{m,*}, A_D^{m,*}) = \left( \frac{\rho + 2\beta\Lambda - \sqrt{4\beta\eta\Lambda(\alpha+\chi(\theta\delta_\ell+(1-\theta)\delta_h)) + \rho^2}}{2\alpha\beta}, \frac{\sqrt{4\beta\eta\Lambda(\alpha+\chi(\theta\delta_\ell+(1-\theta)\delta_h)) + \rho^2} - \rho}{2\beta(\alpha+\chi(\theta\delta_\ell+(1-\theta)\delta_h))} \right).$$

Given this equilibrium, our goal is to minimize the expected number of overdoses through an optimal accessibility policy:

$$\min_{\theta\in[0,1]} \quad \mathcal{D}_D^m(\theta) := \chi\left(\theta\delta_\ell + (1-\theta)\delta_h\right) A_D^{m,*}. \tag{EC.1.2}$$

To analyze this objective, we define the following expressions:

$$\begin{aligned} \mathcal{U}_h &= \alpha^2 - \beta\Lambda + \sqrt{\left(\alpha(\alpha+\gamma+\eta) - \beta\Lambda + \chi(\alpha+\eta)\delta_h\right)^2 + 4\beta\eta\Lambda(\alpha+\chi\delta_h)} + \alpha(\gamma+\eta), \\ \mathcal{V}_h &= \chi\delta_h \left( \frac{\beta\Lambda(\eta-\alpha) + \alpha(\alpha+\eta)(\alpha+\gamma+\eta) + \chi(\alpha+\eta)^2\delta_h}{\sqrt{\left(\alpha(\alpha+\gamma+\eta) - \beta\Lambda + \chi(\alpha+\eta)\delta_h\right)^2 + 4\beta\eta\Lambda(\alpha+\chi\delta_h)}} \right), \\ \mathcal{U}_\ell &= \alpha^2 - \beta\Lambda + \sqrt{\left(\alpha(\alpha+\gamma+\eta) - \beta\Lambda + \chi(\alpha+\eta)\delta_\ell\right)^2 + 4\beta\eta\Lambda(\alpha+\chi\delta_\ell)} + \alpha(\gamma+\eta), \\ \mathcal{V}_\ell &= \chi\delta_\ell \left( \frac{\beta\Lambda(\eta-\alpha) + \alpha(\alpha+\eta)(\alpha+\gamma+\eta) + \chi(\alpha+\eta)^2\delta_\ell}{\sqrt{\left(\alpha(\alpha+\gamma+\eta) - \beta\Lambda + \chi(\alpha+\eta)\delta_\ell\right)^2 + 4\beta\eta\Lambda(\alpha+\chi\delta_\ell)}} \right). \end{aligned}$$

THEOREM EC.1.1 **(Optimal Accessibility under Mass Action Incidence)**. *The solution to problem (EC.1.2) follows the structure below:*

1. ***Full accessibility*** $(\theta = 1)$ ***is optimal*** *if any of the following holds:*

a. $\beta\Lambda \leq \gamma(\alpha+\eta)$;

b. $\beta\Lambda > \gamma(\alpha+\eta)$ *and* $\mathcal{V}_h \leq \mathcal{U}_h$;

c. $\beta\Lambda > \gamma(\alpha+\eta)$, $\mathcal{V}_h > \mathcal{U}_h$, $\mathcal{V}_\ell < \mathcal{U}_\ell$, *and* $\mathcal{D}_D^m(\theta=1) < \mathcal{D}_D^m(\theta=0)$.

2. ***No accessibility*** $(\theta = 0)$ ***is optimal*** *if any of the following holds:*

a. $\beta\Lambda > \gamma(\alpha+\eta)$ *and* $\mathcal{V}_\ell \geq \mathcal{U}_\ell$;

b. $\beta\Lambda > \gamma(\alpha+\eta)$, $\mathcal{V}_h > \mathcal{U}_h$, $\mathcal{V}_\ell < \mathcal{U}_\ell$, *and* $\mathcal{D}_D^m(\theta=0) \leq \mathcal{D}_D^m(\theta=1)$.

While the specific conditions differ slightly from those in Theorem 2 under standard incidence $\beta S(t)A(t)/N(t)$, the overall structure of the solution and the key insights remain consistent.

## EC.2. Equilibrium of the D-SAS and D-SAS-M Models

Let $\Omega=\sqrt{\zeta}$, where $\zeta=(\alpha-\beta+\gamma+\eta+\chi(1-\theta)\delta_h+\chi\theta\delta_\ell)^2+4\beta\eta>0$. There are two sets of solutions for equations

$$\begin{cases}\Lambda-(\alpha+\eta)\,S_D^*-\beta\dfrac{S_D^*A_D^*}{S_D^*+A_D^*}+\gamma A_D^*=0,\\ \eta S_D^*+\beta\dfrac{S_D^*A_D^*}{S_D^*+A_D^*}-(\alpha+\gamma+\chi\theta\delta_\ell+\chi(1-\theta)\delta_h)\,A_D^*=0,\end{cases}$$

including

$$\begin{aligned}S_{D,1}^*&=\frac{\alpha\Lambda\,(\alpha+\beta+\gamma+\eta-\Omega)-\Lambda\chi\,((\theta-1)\delta_h-\theta\delta_\ell)\,(\beta-\gamma+\eta+(\theta-1)\chi\delta_h-\Omega-\theta\chi\delta_\ell)}{2\,(\alpha^2\beta+\chi\,((\theta-1)\delta_h-\theta\delta_\ell)\,(\alpha(\alpha-\beta+\gamma+\eta)+\chi(\alpha+\eta)\,(\theta\delta_\ell-(\theta-1)\delta_h)))},\\ A_{D,1}^*&=\frac{2\eta\Lambda}{-(\theta-1)\chi(\alpha+2\eta)\delta_h+\alpha\,(\alpha-\beta+\gamma+\eta+\Omega)+\theta\chi(\alpha+2\eta)\delta_\ell};\\ S_{D,2}^*&=\frac{\Lambda\,(\alpha\,(\alpha+\beta+\gamma+\eta+\Omega)-\chi\,((\theta-1)\delta_h-\theta\delta_\ell)\,(\beta-\gamma+\eta+(\theta-1)\chi\delta_h+\Omega-\theta\chi\delta_\ell))}{2\,(\alpha^2\beta+\chi\,((\theta-1)\delta_h-\theta\delta_\ell)\,(\alpha(\alpha-\beta+\gamma+\eta)+\chi(\alpha+\eta)\,(\theta\delta_\ell-(\theta-1)\delta_h)))},\\ A_{D,2}^*&=\frac{2\eta\Lambda}{-(\theta-1)\chi(\alpha+2\eta)\delta_h+\alpha\,(\alpha-\beta+\gamma+\eta-\Omega)+\theta\chi(\alpha+2\eta)\delta_\ell}.\end{aligned}$$

Notice that

$$\frac{S_{D,2}^*}{A_{D,2}^*}=\frac{\alpha-\beta+\gamma-\eta+\delta_h(\chi-\theta\chi)-\Omega+\theta\chi\delta_\ell}{2\eta}<0 \text{ and } \frac{S_{D,1}^*}{A_{D,1}^*}=\frac{\alpha-\beta+\gamma-\eta+\delta_h(\chi-\theta\chi)+\Omega+\theta\chi\delta_\ell}{2\eta}>0$$

because of $(\alpha-\beta+\gamma+\eta-\theta\chi\delta_h+\chi\delta_h+\theta\chi\delta_\ell)^2-\zeta=-4\beta\eta<0$. Given that $S_{D,2}^*$ and $A_{D,2}^*$ have opposite signs, that pair cannot represent a biologically valid equilibrium. On the other hand, it is easy to see that $A_{D,1}^*>0$, and thus $S_{D,1}^*>0$ due to $\frac{S_{D,1}^*}{A_{D,1}^*}>0$. Hence, the only admissible equilibrium for D-SAS model is $\left(S_D^*,A_D^*\right)=\left(S_{D,1}^*,A_{D,1}^*\right)$.

Let $\Omega_M=\sqrt{\zeta_M}$, where $\zeta_M=(\alpha-\beta+\gamma+\eta+\chi(1-\theta)\delta_h+(\chi+\Delta)\theta\delta_\ell)^2+4\beta\eta>0$. Similarly, the only admissible equilibrium for D-SAS-M model is

$$\begin{aligned}S_{D,M}^*&=\frac{\alpha\Lambda\,(\alpha+\beta+\gamma+\eta-\Omega_M)+\Lambda\,((\theta-1)\chi\delta_h-\theta(\Delta+\chi)\delta_\ell)\,(-\beta+\gamma-\eta+\delta_h(\chi-\theta\chi)+\Omega_M+\theta(\Delta+\chi)\delta_\ell)}{2\,(\alpha^2\beta+((\theta-1)\chi\delta_h-\theta(\Delta+\chi)\delta_\ell)\,(\alpha(\alpha-\beta+\gamma+\eta)+(\alpha+\eta)\,(\delta_h(\chi-\theta\chi)+\theta(\Delta+\chi)\delta_\ell)))},\\ A_{D,M}^*&=\frac{2\eta\Lambda}{-(\theta-1)\chi(\alpha+2\eta)\delta_h+\alpha\,(\alpha-\beta+\gamma+\eta+\Omega_M)+\theta(\alpha+2\eta)(\Delta+\chi)\delta_\ell}.\end{aligned}$$

## EC.3. The Impact of Moral Hazard on Overdose Mortality

We define

$$\begin{aligned}\mathcal{T}_1&=(\theta-1)\chi\delta_h+\mathcal{T}_2-\theta\chi\delta_\ell,\\ \mathcal{T}_2&=\sqrt{(\alpha-\beta+\gamma+\eta+\chi(1-\theta)\delta_h+\chi\theta\delta_\ell)^2+4\beta\eta},\\ \Delta^*&=\frac{2\eta(\alpha+\beta+\gamma)+(\alpha-\beta+\gamma)^2+\eta^2-2\chi(\alpha-\beta+\gamma+\eta)\,((\theta-1)\delta_h-\theta\delta_\ell)}{2\theta\delta_\ell(\beta-\alpha-\gamma-\eta)}.\end{aligned}$$

PROPOSITION EC.3.1 **(The Impact of Moral Hazard on Overdose Mortality)**. *For a fixed accessibility $\theta$, we have:*

*Case 1. When $\beta\le\bar{\beta}$, $\mathcal{D}'_{D,M}(\Delta)>0$.*

*Case 2. When $\beta>\bar{\beta}$,*

*a. When $\mathcal{T}_1\le 0$, $\mathcal{D}'_{D,M}(\Delta)<0$;*

*b. When $\mathcal{T}_1>0$, $\mathcal{D}'_{D,M}(\Delta)>0$ when $0<\Delta\le\Delta^*$ and $\mathcal{D}'_{D,M}(\Delta)<0$ when $\Delta>\Delta^*$.*

Proposition EC.3.1 clearly demonstrates that moral hazard could decrease overdose mortality. Although moral hazard is typically viewed as harmful because it encourages riskier opioid use. However, in some cases, the resulting increase in overdose deaths may disrupt OUD transmission, ultimately reducing its long-term prevalence and fatalities.

## EC.4. Parameter Estimations

### EC.4.1. Data Collection

We use the CDC WONDER database to obtain mortality data. To identify deaths attributable to opioid overdoses, we group the data by `Year` and `Single-Year Ages`. For `Underlying Cause of Death`, we first select `UCD - Drug/Alcohol Induced Causes`, and then specify codes `X40-X44`, `X60-X64`, `X85`, and `Y10-Y14`, which correspond to drug overdose deaths. Within `Multiple Cause of Death` category, we further select codes `T40.0 (Opium)`, `T40.1 (Heroin)`, `T40.2 (Other opioids)`, `T40.3 (Methadone)`, `T40.4 (Other synthetic narcotics)`, and `T40.6 (Other and unspecified narcotics)` (Doleac and Mukherjee 2022) under `MCD - ICD-10 Codes`, which specifically identify overdose deaths involving opioids. This approach enables us to extract the number of opioid overdose deaths by age for each year, thereby allowing us to quantify annual opioid overdose mortality among individuals aged 12 and older in the U.S. from 2010 to 2019.

We also use the CDC WONDER database to obtain age-specific all-cause mortality data in the U.S. from 2010 to 2019. After grouping the data by `Year` and `Single-Year Ages`, we select `All Causes of Death` under `UCD - ICD-10 Codes` in `Underlying Cause of Death` category to extract the corresponding mortality counts. The database also returns a `Population` column, which records the total U.S. population by age for each year. Using this column, we calculate the total population $N(t)$ aged 12 years and older from 2010 to 2019.

Given the inherent challenges in directly observing and statistically quantifying $A(t)$, Keyes et al. (2022) use three multiplier approaches to estimate the prevalence of OUD among individuals aged 12 and older in the U.S. from 2010 to 2019, aiming to address potential underestimation of its true magnitude. In our study, we take the mortality-based multiplier adjustment they describe (the second multiplier adjustment in Keyes et al. (2022)) as the benchmark estimate for $A(t)$, as it relies on comprehensive national vital statistics and thus offers an objective and consistent data source. This method may also help mitigate some of the underreporting biases inherent in survey data, making it a reasonable comparator. Moreover, Keyes et al. (2022) suggest that the mortality-based multiplier adjustment could be viewed as providing a potential upper bound for the estimate of $A(t)$, thereby indicating the more severe potential trajectory of the opioid crisis and helping ensure that decision-makers remain aware of the associated risks. We also report sensitivity analyses for two additional multiplier approaches in Appendix EC.4.4.

The sequence $S(t)$ is subsequently obtained by subtracting the estimated OUD population $A(t)$ from the total U.S. population aged 12 and over for each corresponding year. Prior to estimating model parameters, we apply Gaussian kernel smoothing to all time series data to reduce potential noise and improve estimation accuracy.

For notational convenience, we define $t_0 = 2010$, $t_1 = 2011$, $\cdots$, $t_T = 2019$, and introduce the time index set $\mathbb{T}_T := \{t_0, t_1, \ldots, t_T\}$ $(T = 9)$.

## EC.4.2. Estimations

*Estimation of inflow rate* $\Lambda$. We consider individuals who reach the age of 12 in each year as the inflow entering the system. Based on the data collected from CDC WONDER in Appendix EC.4.1, we calculate that the average number of individuals turning 12 years old annually between 2010 and 2019 is 4,142,545. Accordingly, we estimate the entry rate as $\Lambda = 4{,}142{,}545$ persons/year.

*Estimation of natual death rate* $\alpha$. Let $\mathbf{D}_\alpha(t)$ and $\mathbf{D}(t)$ denote the number of deaths unrelated and related to opioid overdose, respectively. Then we have $\mathbf{D}_\alpha(t) = $ Total Deaths in Year $t - \mathbf{D}(t)$ for the SAS family of models. Next, we have a regression function:

$$\mathbf{D}_\alpha(t) = \alpha(S(t) + A(t)) = \alpha N(t),$$

where $N(t)$ is the total population in the U.S. in year $t$. By the least squares method, the corresponding loss function is

$$\min_{\alpha} \quad L(\alpha) = \sum_{t \in \mathbb{T}_T} \left(\mathbf{D}_\alpha(t) - \alpha N(t)\right)^2. \tag{EC.4.3}$$

By solving problem (EC.4.3), we obtain $\alpha = 0.009627$.

*Estimation of overall mortality rate regarding opioid overdose.* In the SAS and D-SAS models, the overall mortality rate due to opioid overdose, given by $\chi(1-\theta)\delta_h + \chi\theta\delta_\ell$, can be denoted as $\phi$. In the SAS-M and D-SAS-M models, the overall mortality rate, accounting for the effect of moral hazard, is given by $\chi(1-\theta)\delta_h + \chi\theta\delta_\ell + \Delta\theta\delta_\ell$, and is likewise denoted by $\phi$. Thus, the regression function

$$\mathbf{D}(t) = \phi A(t)$$

holds for all SAS family of models. By the least squares method, the corresponding loss function is

$$\min_{\alpha} \quad L(\phi) = \sum_{t \in \mathbb{T}_T} \left(\mathbf{D}(t) - \phi A(t)\right)^2. \tag{EC.4.4}$$

By solving problem (EC.4.4), we obtain $\phi = 0.003338$.

*Estimation of tranmission rate* $\beta$. By rearranging the discrete version of the D-SAS and D-SAS-M models, we have:

$$\begin{cases} \Lambda - \alpha S(t) + \gamma A(t) - S(t+1) + S(t) - \eta S(t) = \beta \dfrac{S(t)A(t)}{N(t)}, \\ A(t+1) - A(t) + (\alpha + \gamma + \phi) A(t) - \eta S(t) = \beta \dfrac{S(t)A(t)}{N(t)}. \end{cases}$$

Let

$$\begin{aligned} Y_1(t) &= \Lambda - \alpha S(t) + \gamma A(t) - S(t+1) + S(t) - \eta S(t), \\ Y_2(t) &= A(t+1) - A(t) + (\alpha + \gamma + \phi) A(t) - \eta S(t), \\ X(t) &= \frac{S(t)A(t)}{N(t)}. \end{aligned}$$

By the least squares method, the corresponding loss function is

$$\min_{\beta} \quad L(\beta) = \sum_{t \in \mathbb{T}_{T-1}} \sum_{i=1,2} \left(Y_i(t) - \beta X(t)\right)^2. \tag{EC.4.5}$$

Notice that the time set in problem (EC.4.5) is $\mathbb{T}_{T-1}$ instead of $\mathbb{T}_T$ because applying a first-order difference to a time series results in the loss of one observation. Then, by solving problem (EC.4.5), we obtain $\beta = 0.075914$.

Note that in our linear estimations of parameters $\alpha$, $\phi$, and $\beta$, the associated $p$-values are all below 0.05, indicating that these estimates are statistically significant and valid.

### EC.4.3. Model Validation

After calibrating all the parameters, we assess the goodness of fit for the SAS family of models by substituting the calibrated values into the system and regenerating the trajectories of $S(t)$, $A(t)$, and $\mathbf{D}(t)$. Table EC.1 below reports the mean absolute percentage error (MAPE) between the model-generated trajectories and the corresponding training data for $S(t)$, $A(t)$, and $\mathbf{D}(t)$. Figure EC.4.1 presents the trajectories of $S(t)$, $A(t)$, and $\mathbf{D}(t)$ obtained from the model, along with the corresponding time-series data used for parameter estimation.

**Table EC.1 MAPE results for the SAS family of models.**

| | $S(t)$ | $A(t)$ | $\mathbf{D}(t)$ |
|---|---|---|---|
| SAS and SAS-M models | 0.005679 | 0.209629 | 0.231883 |
| D-SAS and D-SAS-M models | 0.005445 | 0.041470 | 0.093064 |

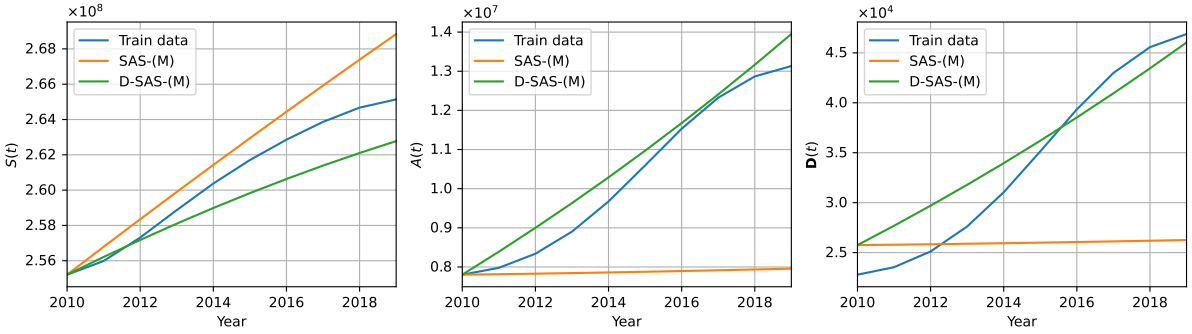


**Figure EC.4.1 Trajectories of $S(t)$, $A(t)$, and $\mathbf{D}(t)$ obtained from the models with the time-series data used for parameter estimation.**

Table EC.1 shows that the D-SAS-(M) models yield consistently small MAPE values, suggesting that this framework effectively captures the dynamics of the U.S. opioid crisis. In contrast, the SAS-(M) models without social transmission exhibit relatively large MAPE values for $A(t)$ and $\mathbf{D}(t)$. Figure EC.4.1 also provides a clear visual indication that incorporating social contagion improves the models' goodness of fit. This discrepancy arises because the training data for $A(t)$ show rapid growth that the linear SAS models cannot adequately track, thus further amplifying the error in $\mathbf{D}(t)$ under a fixed overall mortality rate (see the right plot in Figure EC.4.1). In contrast, the D-SAS-(M) models with interaction terms enable $A(t)$ to exhibit rapid nonlinear growth, which allows the model-generated trajectory of $\mathbf{D}(t)$ to achieve a closer fit to the training data under a fixed overall mortality rate.

### EC.4.4. Sensitivity Analyses

Keyes et al. (2022) suggests three multiplier approaches to estimate the prevalence of OUD. In addition to the mortality-based multiplier adjustment we used in Section EC.4.1, in this section, we further examine the two other time series of $A(t)$ reported in Keyes et al. (2022): one based on survey data (the first adjustment in Keyes et al. 2022) and one derived from mortality data with multiplier correction (the third adjustment in Keyes et al. 2022).

Table EC.2 reports the estimates of $\alpha$, $\beta$, and $\chi$ under the two alternative specifications of $A(t)$. In both adjustments, $\alpha$ exceeds $\beta$, suggesting that social contagion contributed only modestly to opioid addiction during 2010–2019, in contrast to the conclusion from our benchmark model. This discrepancy can be explained by the markedly different dynamics of $A(t)$ across the benchmark and adjusted series. In the benchmark, $A(t)$ shows a largely monotonic upward trajectory (see the blue line in the middle panel of Figure EC.4.1), while in the two adjustments, it first increases and then decreases. Such a pattern offers limited flexibility for identifying the fixed OUD transmission rate $\beta$ and therefore tends to reduce its estimated magnitude. Although the estimated $\beta$ is relatively small, we believe that the risk of OUD driven by social interactions should not be overlooked, especially considering that the COVID-19 pandemic appears to have amplified the impact of this channel of addiction (Janssen et al. 2023). Finally, since the moral hazard $\Delta$ remains below the threshold $\bar{\Delta}$ under both adjustments (see the last column of Table EC.2), the optimal accessibility of naloxone is consistently 1 across all four models.

**Table EC.2 Some estimates under additional two adjustments of $A(t)$.**

| | $\alpha$ | $\beta$ | $\chi$ ((D)-SAS) | $\chi$ ((D)-SAS-M) | $\bar{\Delta}-\Delta$ ((D)-SAS-M) |
|---|---|---|---|---|---|
| Survey data, multiplier | 0.009627 | 0.002602 | 0.004097 | 0.004092 | 0.024512 |
| Mortality data, multiplier with correction | 0.009627 | 0.007509 | 0.005621 | 0.005615 | 0.033633 |

Table EC.3 reports the MAPE values between the model-generated trajectories and the corresponding training data for $S(t)$, $A(t)$, and $\mathbf{D}(t)$ under the two alternative specifications of $A(t)$. We observe that, in Table EC.3, the MAPE values for $S(t)$ and $A(t)$ are relatively small, whereas the MAPE values for $\mathbf{D}(t)$ are substantially larger. This limitation likely reflects the difficulty of our fixed-coefficient models in capturing the successive waves of the opioid epidemic between 2010 and 2019. As noted by Keyes et al. (2022) and Mattson (2022), 2015 marked a critical inflection point characterized by the rapid escalation of synthetic opioid abuse—a dynamic not captured in our framework. As a result, the models may underestimate opioid overdose deaths in back-testing and thus increase the errors. We leave the development of a dynamic model with time-varying coefficients, better suited to capturing structural shifts, for future research.

## EC.5. Parameters used in Numerical Examples

Please see Table EC.4, Table EC.5 and Table EC.6.

**Table EC.3 MAPE results under additional two adjustments of $A(t)$.**

| | | $S(t)$ | $A(t)$ | $\mathbf{D}(t)$ |
|---|---|---|---|---|
| Survey data, multiplier | SAS and SAS-M models | 0.004522 | 0.032701 | 0.257574 |
| | D-SAS and D-SAS-M models | 0.004787 | 0.031967 | 0.254297 |
| Mortality data, multiplier with correction | SAS and SAS-M models | 0.004406 | 0.022509 | 0.233969 |
| | D-SAS and D-SAS-M models | 0.004976 | 0.023721 | 0.224055 |

**Table EC.4 Parameter values used in Figure 3: $\eta = 0.001$, $\gamma = 0.01$, $\chi = 0.02$, $\alpha = 0.006$, $\beta = 0.025$, and $\Lambda = 200{,}000$.**

| | $\delta_h$ | $\delta_\ell$ | $\bar{\delta}$ | $\beta - \bar{\beta}$ |
|---|---|---|---|---|
| Left plot | 0.90 | 0.10 | 0.5125 | 0.008 |
| Right plot | 0.80 | 0.38 | 0.5125 | 0.008 |

**Table EC.5 Parameter values used in Figure 5: $\eta = 0.0003$, $\gamma = 0.016$, $\alpha = 0.006$, and $\Lambda = 200{,}000$.**

| | $\beta$ | $\beta - \bar{\beta}$ |
|---|---|---|
| Left plot | 0.025 | 0.0027 |
| Right plot | Less than $\bar{\beta} = 0.0223$ suffices | $< 0$ |

**Table EC.6 Parameter values used in Figure 7: $\eta = 0.001$, $\gamma = 0.001$, $\alpha = 0.006$, $\beta = 0.025$, and $\Lambda = 200{,}000$.**

| | $\delta_h$ | $\delta_\ell$ | $\chi$ | $\bar{\delta}$ | $\bar{\delta}_M$ | $\bar{\Delta}$ |
|---|---|---|---|---|---|---|
| Left plot (Case 1d) | 0.85 | 0.15 | 0.0250 | 0.457647 | 0.440045 | 0.116667 |
| Left plot (Case 2d) | 0.85 | 0.15 | 0.0250 | 0.457647 | 0.286029 | 0.116667 |
| Right plot (Case 2e) | 0.55 | 0.40 | 0.0125 | 0.915294 | 0.269204 | 0.004688 |
| Right plot (Case 1e) | 0.55 | 0.40 | 0.0125 | 0.915294 | 0.226558 | 0.004688 |

## EC.6. Proofs of Theoretical Results

*Proof of Proposition 1.* Recall that the steady-state mortality is given by

$$\mathcal{D}(\theta) = \frac{\eta\Lambda\left[(1-\theta)\chi\delta_h + \theta\chi\delta_\ell\right]}{\alpha(\alpha+\gamma+\eta) + \chi(\alpha+\eta)\left[\theta\delta_\ell - (\theta-1)\delta_h\right]}.$$

Differentiating with respect to $\theta$, we obtain

$$\mathcal{D}'(\theta) = -\frac{\alpha\eta\Lambda\chi(\alpha+\gamma+\eta)(\delta_h - \delta_\ell)}{\left[\alpha(\alpha+\gamma+\eta) - (\theta-1)\chi(\alpha+\eta)\delta_h + \theta\chi(\alpha+\eta)\delta_\ell\right]^2} < 0,$$

since $\delta_h > \delta_\ell$.

Thus, the mortality function $\mathcal{D}(\theta)$ is strictly decreasing in $\theta$, and the minimum is attained at $\theta^* = 1$. Q.E.D.

*Proof of Theorem 1.* Recall that

$$\mathcal{D}_M(\theta) = \frac{\eta\Lambda\left((1-\theta)\chi\delta_h + \theta(\Delta+\chi)\delta_\ell\right)}{\alpha(\alpha+\gamma+\eta) + (\alpha+\eta)\left(\delta_h(\chi-\theta\chi) + \theta(\Delta+\chi)\delta_\ell\right)}.$$

Then, we have

$$\mathcal{D}'_M(\theta) = -\frac{\alpha\eta\Lambda(\alpha+\gamma+\eta)\left(\chi\delta_h-(\Delta+\chi)\delta_\ell\right)}{\left(\alpha(\alpha+\gamma+\eta)-(\theta-1)\chi(\alpha+\eta)\delta_h+\theta(\alpha+\eta)(\Delta+\chi)\delta_\ell\right)^2},$$

where the sign of $\mathcal{D}'_M(\theta)$ depends on the sign of $\chi\delta_h-(\Delta+\chi)\delta_\ell$. When $\Delta<\bar{\Delta}=\frac{\chi(\delta_h-\delta_\ell)}{\delta_\ell}$, we have $(\chi\delta_h-(\Delta+\chi)\delta_\ell)>0$ and thus $\theta^*=1$. When $\Delta>\bar{\Delta}$, however, we get that $(\chi\delta_h-(\Delta+\chi)\delta_\ell)<0$ and thus $\theta^*=0$. In particular, when $\Delta=\bar{\Delta}$, $\mathcal{D}'_M(\theta)=0$ and, therefore, any accessibility is optimal. For clarity and consistency, we directly set $\theta^*=0$ in this case. Q.E.D.

*Proof of Theorem 2.* Recall that

$$A^*_D = \frac{2\eta\Lambda}{-(\theta-1)\chi(\alpha+2\eta)\delta_h+\alpha\left(\bar{\beta}-\beta+\Omega\right)+\theta\chi(\alpha+2\eta)\delta_\ell},$$

where

$$\Omega=\sqrt{2\eta(\alpha+\beta+\gamma)+(\alpha-\beta+\gamma)^2+\eta^2-\chi\left((\theta-1)\delta_h-\theta\delta_\ell\right)\left(2(\bar{\beta}-\beta)+\delta_h(\chi-\theta\chi)+\theta\chi\delta_\ell\right)}.$$

Then, we have

$$\mathcal{D}_D(\theta) = \frac{((1-\theta)\chi\delta_h+\theta\chi\delta_\ell)2\eta\Lambda}{-(\theta-1)\chi(\alpha+2\eta)\delta_h+\alpha\left(\bar{\beta}-\beta+\Omega\right)+\theta\chi(\alpha+2\eta)\delta_\ell},$$

and

$$\mathcal{D}'_D(\theta) = \frac{P(\theta)}{\Omega\left(-(\theta-1)\chi(\alpha+2\eta)\delta_h+\alpha\left(\bar{\beta}-\beta+\Omega\right)+\theta\chi(\alpha+2\eta)\delta_\ell\right)^2},$$

where $P(\theta)=-2\alpha\eta\Lambda\chi\left(\delta_h-\delta_\ell\right)\left(\theta\chi\delta_h-\chi\delta_h+\Omega-\theta\chi\delta_\ell\right)\left(\bar{\beta}-\beta-\theta\chi\delta_h+\chi\delta_h+\Omega+\theta\chi\delta_\ell\right)$.

Next, we focus our attention on the derivative of $P(\theta)$:

$$P'(\theta)=\frac{2\alpha\eta\Lambda\chi^2\left(\delta_h-\delta_\ell\right)^2(\bar{\beta}-\beta)\left(\bar{\beta}-\beta-\theta\chi\delta_h+\chi\delta_h+\Omega+\theta\chi\delta_\ell\right)}{\Omega}.$$

Note that the term $\left(\bar{\beta}-\beta-\theta\chi\delta_h+\chi\delta_h+\Omega+\theta\chi\delta_\ell\right)$ in the numerator in $P'(\theta)$ is strictly positive since

$$\Omega^2-(\bar{\beta}-\beta-\theta\chi\delta_h+\chi\delta_h+\theta\chi\delta_\ell)^2=4\beta\eta>0.$$

Thus, the sign of $P'(\theta)$ only depends on the sign of $(\bar{\beta}-\beta)$. We, therefore, consider the following three cases:

Case 1: If $\beta<\bar{\beta}=\alpha+\gamma+\eta$, $P(\theta)$ monotonically increases.

Case 2: If $\beta=\bar{\beta}$, $P(\theta)$ is a constant.

Case 3: If $\beta>\bar{\beta}$, $P(\theta)$ monotonically decreases.

From the above three cases, we know that $\mathcal{D}'_D(\theta)=0$ has at most one solution when $\beta\neq\bar{\beta}$.

Next, we analyze each of the above cases separately.

Case 1. When $\beta<\bar{\beta}$, then $P'(\theta)>0$ and $P(\theta)$ is increasing. Note that

$$P(\theta=1)=2\alpha\eta\Lambda\chi\left(\delta_h-\delta_\ell\right)\mathcal{Y}_1\mathcal{Y}_2,$$

where

$$\mathcal{Y}_1=\left(\chi\delta_\ell-\sqrt{2\eta(\alpha+\beta+\gamma)+(\alpha-\beta+\gamma)^2+\eta^2+\chi\delta_\ell\left(2(\bar{\beta}-\beta)+\chi\delta_\ell\right)}\right),$$

$$\mathcal{Y}_2=\left(\bar{\beta}-\beta+\sqrt{2\eta(\alpha+\beta+\gamma)+(\alpha-\beta+\gamma)^2+\eta^2+\chi\delta_\ell\left(2(\bar{\beta}-\beta)+\chi\delta_\ell\right)}+\chi\delta_\ell\right).$$

It is easy to see that when $\beta<\bar{\beta}$, then $\mathcal{Y}_1<0$. Additionally, because

$$\left(2\eta(\alpha+\beta+\gamma)+(\alpha-\beta+\gamma)^2+\eta^2+\chi\delta_\ell\left(2(\bar{\beta}-\beta)+\chi\delta_\ell\right)\right)-\left(\bar{\beta}-\beta+\chi\delta_\ell\right)^2=4\beta\eta>0,$$

we have $\mathcal{Y}_2>0$. Therefore, $P(\theta=1)<0$ and thus $P(\theta)<0$ for $\theta\in[0,1]$. Thus, $\mathcal{D}_D(\theta)$ is decreasing and thereby, $\theta^*=1$.

Case 2. When $\beta = \bar{\beta}$, then $P(\theta)$ can be simplified to $-8\alpha\eta^2\Lambda\chi\bar{\beta}\,(\delta_h - \delta_\ell) < 0$. In this case, $\mathcal{D}'_D(\theta) < 0$ and thus $\mathcal{D}_D(\theta)$ is decreasing and $\theta^* = 1$.

Case 3. When $\beta > \bar{\beta}$, then $P'(\theta) < 0$ and thus $P(\theta)$ is decreasing. Note that in this case,

$$P(\theta = 0) = 2\alpha\eta\Lambda\chi\,(\delta_h - \delta_\ell)\,\mathcal{X}_1\mathcal{X}_2,$$

where

$$\begin{aligned}\mathcal{X}_1 &= \left(\chi\delta_h - \sqrt{2\eta(\alpha+\beta+\gamma) + (\alpha-\beta+\gamma)^2 + \eta^2 + \chi\delta_h\left(2(\bar{\beta}-\beta) + \chi\delta_h\right)}\right),\\ \mathcal{X}_2 &= \left(\bar{\beta} - \beta + \sqrt{2\eta(\alpha+\beta+\gamma) + (\alpha-\beta+\gamma)^2 + \eta^2 + \chi\delta_h\left(2(\bar{\beta}-\beta) + \chi\delta_h\right)} + \chi\delta_h\right).\end{aligned} \tag{EC.6.6}$$

Importantly, even when $\beta > \bar{\beta}$, then $\mathcal{X}_2, \mathcal{Y}_2 \geq 0$ , because

$$\left(2\eta(\alpha+\beta+\gamma) + (\alpha-\beta+\gamma)^2 + \eta^2 + \chi\delta_h\left(2(\bar{\beta}-\beta) + \chi\delta_h\right)\right) - \left(\bar{\beta} - \beta + \chi\delta_h\right)^2 = 4\beta\eta > 0;$$

$$\left(2\eta(\alpha+\beta+\gamma) + (\alpha-\beta+\gamma)^2 + \eta^2 + \chi\delta_\ell\left(2(\bar{\beta}-\beta) + \chi\delta_\ell\right)\right) - \left(\bar{\beta} - \beta + \chi\delta_\ell\right)^2 = 4\beta\eta > 0.$$

Now there could be three cases:

Case 3.1. When $P(\theta = 0) < 0$ (i.e., $\mathcal{X}_1 < 0 \Leftrightarrow (\bar{\beta}-\beta)^2 + 4\beta\eta + 2\chi\delta_h(\bar{\beta}-\beta) > 0 \Leftrightarrow \delta_h < \bar{\delta}$), then $\mathcal{D}_D(\theta)$ is decreasing and thus $\theta^* = 1$.

Case 3.2. When $P(\theta = 0) > 0$ and $P(\theta = 1) < 0$ (i.e., $\mathcal{X}_1 > 0$ and $\mathcal{Y}_1 < 0 \Leftrightarrow (\bar{\beta}-\beta)^2 + 4\beta\eta + 2\chi\delta_h(\bar{\beta}-\beta) < 0$ and $(\bar{\beta}-\beta)^2 + 4\beta\eta + 2\chi\delta_\ell(\bar{\beta}-\beta) > 0 \Leftrightarrow \delta_\ell < \bar{\delta} < \delta_h$), $\mathcal{D}(\theta)$ first increases and then decreases over the interval $[0,1]$. Thus, $\theta^* = \arg\min_{\theta\in\{0,1\}} \mathcal{D}_D(\theta)$ considering that the optimal solution can only exist at the extreme values. Note that when $\mathcal{D}_{D,M}(\theta = 0) = \mathcal{D}_{D,M}(\theta = 1)$, we set $\theta^* = 0$ for convenience.

Case 3.3. When $P(\theta = 1) > 0$ (i.e., $\mathcal{Y}_1 > 0 \Leftrightarrow (\bar{\beta}-\beta)^2 + 4\beta\eta + 2\chi\delta_\ell(\bar{\beta}-\beta) < 0 \Leftrightarrow \delta_\ell > \bar{\delta}$), $\mathcal{D}_D(\theta)$ is increasing and thus $\theta^* = 0$.

Collecting the conditions under which $\theta^* = 1$ and $\theta^* = 0$ yields the desired characterization as stated. Q.E.D.

*Proof of Theorem 3.* We begin by examining the special case where $\Delta = \bar{\Delta}$. In this case, the D-SAS-M model becomes independent of the accessibility level $\theta$, as the life-saving benefits of naloxone exactly offset the negative impact of moral hazard. The optimal solution is therefore not unique and may lie anywhere in the interval $[0,1]$. For consistency with the rest of the analysis, we adopt zero accessibility as the default choice.

We now proceed under the assumption that $\Delta \neq \bar{\Delta}$. Recall that

$$A^*_{D,M} = \frac{2\eta\Lambda}{-(\theta-1)\chi(\alpha+2\eta)\delta_h + \alpha\left(\bar{\beta}-\beta+\Omega_M\right) + \theta(\alpha+2\eta)(\Delta+\chi)\delta_\ell},$$

where

$$\Omega_M = \sqrt{(\bar{\beta}-\beta+\chi(1-\theta)\delta_h + (\chi+\Delta)\theta\delta_\ell)^2 + 4\beta\eta}.$$

Then, we have

$$\mathcal{D}_{D,M}(\theta) = \frac{2\eta\Lambda((1-\theta)\chi\delta_h + \theta(\Delta+\chi)\delta_\ell)}{-(\theta-1)\chi(\alpha+2\eta)\delta_h + \alpha\left(\bar{\beta}-\beta+\Omega_M\right) + \theta(\alpha+2\eta)(\Delta+\chi)\delta_\ell}, \tag{EC.6.7}$$

and

$$\mathcal{D}'_{D,M}(\theta) = \frac{Q(\theta)}{\Omega_M \left(-(\theta-1)\chi(\alpha+2\eta)\delta_h + \alpha\left(\bar{\beta}-\beta+\Omega_M\right) + \theta(\alpha+2\eta)(\Delta+\chi)\delta_\ell\right)^2},$$

where

$$Q(\theta) = -2\alpha\eta\Lambda\left(\chi\delta_h - (\Delta+\chi)\delta_\ell\right)\left((\theta-1)\chi\delta_h + \Omega_M - \theta(\Delta+\chi)\delta_\ell\right)\left(\bar{\beta}-\beta+\delta_h(\chi-\theta\chi)+\Omega_M+\theta(\Delta+\chi)\delta_\ell\right).$$

Therefore,

$$\begin{aligned}
Q'(\theta) &= \frac{2\alpha\eta\Lambda(\bar{\beta}-\beta)\left(\chi\delta_h-(\Delta+\chi)\delta_\ell\right)^2\left(\bar{\beta}-\beta+\delta_h(\chi-\theta\chi)+\Omega_M+\theta(\Delta+\chi)\delta_\ell\right)}{\Omega_M},\\
Q(\theta=0) &= 2\alpha\eta\Lambda\left(\chi\delta_h-(\Delta+\chi)\delta_\ell\right)\mathcal{X}_1\mathcal{X}_2,\\
Q(\theta=1) &= 2\alpha\eta\Lambda\left(\chi\delta_h-(\Delta+\chi)\delta_\ell\right)\mathcal{Y}_{1,M}\mathcal{Y}_{2,M},
\end{aligned}$$

where $\mathcal{X}_1$ and $\mathcal{X}_2$ are defined in (EC.6.6) as well as

$$\mathcal{Y}_{1,M} = \left(-\sqrt{2\eta(\alpha+\beta+\gamma)+(\alpha-\beta+\gamma)^2+\eta^2+(\Delta+\chi)\delta_\ell\left(2(\bar{\beta}-\beta)+(\Delta+\chi)\delta_\ell\right)}+(\Delta+\chi)\delta_\ell\right),$$

$$\mathcal{Y}_{2,M} = \left(\bar{\beta}-\beta+\sqrt{2\eta(\alpha+\beta+\gamma)+(\alpha-\beta+\gamma)^2+\eta^2+(\Delta+\chi)\delta_\ell\left(2(\bar{\beta}-\beta)+(\Delta+\chi)\delta_\ell\right)}+(\Delta+\chi)\delta_\ell\right) > 0.$$

Since $Q'(\theta)=0$ if and only if $\Delta=\bar{\Delta}$, provided that $\bar{\beta}-\beta\neq 0$, the sign of $Q'(\theta)$ depends solely on the sign of $(\bar{\beta}-\beta)$. We therefore consider the following cases:

Case 1: If $\beta<\bar{\beta}=\alpha+\gamma+\eta$, then $Q(\theta)$ monotonically increases.

Case 2: If $\beta=\bar{\beta}$, then $Q(\theta)$ is a constant.

Case 3: If $\beta>\bar{\beta}$, then $Q(\theta)$ monotonically decreases.

From the three cases above, it follows that $\mathcal{D}'_{D,M}(\theta)=0$ has at most one solution when $\beta\neq\bar{\beta}$.

Next, we analyze each of the above cases.

Case 1. When $\beta<\bar{\beta}$, then $Q'(\theta)>0$ so $Q(\theta)$ is increasing. In this case, we have $\mathcal{X}_1,\mathcal{Y}_{1,M}<0$ and $\mathcal{X}_2,\mathcal{Y}_{2,M}>0$. Thus, the sign of $Q(\theta=0)$ and $Q(\theta=1)$ also depends on the sign of $(\chi\delta_h-(\Delta+\chi)\delta_\ell)$. There could be two cases:

Case 1.1. When $\Delta<\bar{\Delta}$, we have $Q(\theta=0),Q(\theta=1)<0$. Thus $\mathcal{D}'_{D,M}(\theta)<0$ and $\theta^*=1$.

Case 1.2. When $\Delta>\bar{\Delta}$, we have $Q(\theta=0),Q(\theta=1)>0$. Thus, $\mathcal{D}'_{D,M}(\theta)>0$ and $\theta^*=0$.

Case 2. When $\beta=\bar{\beta}$, then $Q(\theta)$ is reduced to $-8\alpha\eta^2\Lambda(\alpha+\gamma+\eta)\left(\chi\delta_h-(\Delta+\chi)\delta_\ell\right)$. There could be two cases:

Case 2.1. When $\Delta<\bar{\Delta}$, we have $Q(\theta)<0$. Thus, $\mathcal{D}'_{D,M}(\theta)<0$ and $\theta^*=1$.

Case 2.2. When $\Delta>\bar{\Delta}$, we have $Q(\theta)>0$. Thus, $\mathcal{D}'_{D,M}(\theta)>0$ and $\theta^*=0$.

Case 3. When $\beta>\bar{\beta}$, $Q'(\theta)<0$ and thus $Q(\theta)$ is decreasing. There could be three cases:

Case 3.1. When $Q(\theta=0)\leq 0$:

Case 3.1.1. When $\Delta<\bar{\Delta}$ and $\mathcal{X}_1<0$ (i.e., $(\bar{\beta}-\beta)^2+4\beta\eta+2\chi\delta_h(\bar{\beta}-\beta)>0\Leftrightarrow\delta_h<\bar{\delta}$), we have $Q(\theta)<0$ for all $\theta\in[0,1]$. Thus, $\mathcal{D}'_{D,M}(\theta)<0$ and $\theta^*=1$.

Case 3.1.2. When $\Delta>\bar{\Delta}$ and $\mathcal{X}_1>0$ (i.e., $(\bar{\beta}-\beta)^2+4\beta\eta+2\chi\delta_h(\bar{\beta}-\beta)<0\Leftrightarrow\delta_h>\bar{\delta}$), we have $Q(\theta)<0$ for all $\theta\in[0,1]$. Thus, $\mathcal{D}'_{D,M}(\theta)<0$ and $\theta^*=1$.

Case 3.1.3. When $\mathcal{X}_1=0$ (i.e., $(\bar{\beta}-\beta)^2+4\beta\eta+2\chi\delta_h(\bar{\beta}-\beta)=0\Leftrightarrow\delta_h=\bar{\delta}$), we have $Q(\theta=0)=0$ and $Q(\theta)<0$ for all $\theta\in(0,1]$. Thus, $\theta^*=1$.

Case 3.2. When $Q(\theta=0)>0$ and $Q(\theta=1)<0$, then $\mathcal{D}_{D,M}(\theta)$ first increases and then decreases over the interval $[0,1]$:

Case 3.2.1. When $\Delta<\bar{\Delta}$, $\mathcal{X}_1>0$ (i.e., $(\bar{\beta}-\beta)^2+4\beta\eta+2\chi\delta_h(\bar{\beta}-\beta)<0\Leftrightarrow\delta_h>\bar{\delta}$) and $\mathcal{Y}_{1,M}<0$ (i.e., $(\bar{\beta}-\beta)^2+4\beta\eta+2(\chi+\Delta)\delta_\ell(\bar{\beta}-\beta)>0\Leftrightarrow\delta_\ell<\bar{\delta}_M$), $\theta^*=\arg\min_{\theta\in\{0,1\}}\mathcal{D}_{D,M}(\theta)$ because, in this case, the optimal solution exists only on the boundaries.

Case 3.2.2. When $\Delta>\bar{\Delta}$, $\mathcal{X}_1<0$ (i.e., $(\bar{\beta}-\beta)^2+4\beta\eta+2\chi\delta_h(\bar{\beta}-\beta)>0\Leftrightarrow\delta_h<\bar{\delta}$) and $\mathcal{Y}_{1,M}>0$ (i.e., $(\bar{\beta}-\beta)^2+4\beta\eta+2(\chi+\Delta)\delta_\ell(\bar{\beta}-\beta)<0\Leftrightarrow\delta_\ell>\bar{\delta}_M$), $\theta^*=\arg\min_{\theta\in\{0,1\}}\mathcal{D}_{D,M}(\theta)$ because, in this case, the optimal solution exists only on the boundaries.

Note that when $\mathcal{D}_{D,M}(\theta=0)=\mathcal{D}_{D,M}(\theta=1)$, we set $\theta^*=0$ for convenience.

Case 3.3. When $Q(\theta=1)\geq 0$:

Case 3.3.1. When $\Delta<\bar{\Delta}$ and $\mathcal{Y}_{1,M}>0$ (i.e., $(\bar{\beta}-\beta)^2+4\beta\eta+2(\chi+\Delta)\delta_\ell(\bar{\beta}-\beta)<0\Leftrightarrow\delta_\ell>\bar{\delta}_M$), we have $Q(\theta)>0$ for all $\theta\in[0,1]$. Thus, $\mathcal{D}'_{D,M}(\theta)<0$ and $\theta^*=0$.

Case 3.3.2. When $\Delta>\bar{\Delta}$ and $\mathcal{Y}_{1,M}<0$ (i.e., $(\bar{\beta}-\beta)^2+4\beta\eta+2(\chi+\Delta)\delta_\ell(\bar{\beta}-\beta)>0\Leftrightarrow\delta_\ell<\bar{\delta}_M$), we have $Q(\theta)>0$ for all $\theta\in[0,1]$. Thus, $\mathcal{D}'_{D,M}(\theta)<0$ and $\theta^*=0$.

Case 3.3.3. When $\mathcal{Y}_{1,M}=0$ (i.e., $(\bar{\beta}-\beta)^2+4\beta\eta+2(\chi+\Delta)\delta_\ell(\bar{\beta}-\beta)=0\Leftrightarrow\delta_\ell=\bar{\delta}_M$), we have $Q(\theta=1)=0$ and $Q(\theta)>0$ for all $\theta\in(0,1]$. Thus, $\theta^*=0$.

Collecting the conditions under which $\theta^*=1$ and $\theta^*=0$ yields the desired characterization stated. Q.E.D.

*Proof of Theorem EC.1.1.* The full expression of $\mathcal{D}_D^m(\theta)$ is

$$\mathcal{D}_D^m(\theta)=\frac{2\eta\Lambda\left(\delta_h(\chi-\theta\chi)+\theta\chi\delta_\ell\right)}{\rho+\sqrt{\rho^2+4\beta\eta\Lambda\left(\alpha+\delta_h(\chi-\theta\chi)+\theta\chi\delta_\ell\right)}},$$

and

$$\mathcal{D}_D^{'m}(\theta)=\frac{\mathcal{P}(\theta)}{\left(\rho+\sqrt{\rho^2+4\beta\eta\Lambda\left(\alpha+\delta_h(\chi-\theta\chi)+\theta\chi\delta_\ell\right)}\right)^2},$$

where

$$\begin{aligned}\mathcal{P}(\theta)=&-2\eta\Lambda\chi\left(\delta_h-\delta_\ell\right)\left(\rho+\sqrt{\rho^2+4\beta\eta\Lambda\left(\alpha+\chi(\theta\delta_\ell+(1-\theta)\delta_h)\right)}\right)\\&+2\eta\Lambda\chi\left(\delta_h-\delta_\ell\right)\left(\chi(\theta\delta_\ell+(1-\theta)\delta_h)\left(\eta+\alpha+\frac{\beta\Lambda(\eta-\alpha)+\alpha(\alpha+\eta)(\alpha+\gamma+\eta)+\chi(\alpha+\eta)^2(\theta\delta_\ell+(1-\theta)\delta_h)}{\sqrt{\rho^2+4\beta\eta\Lambda\left(\alpha+\chi(\theta\delta_\ell+(1-\theta)\delta_h)\right)}}\right)\right).\end{aligned}$$

Additionally, we have

$$\mathcal{P}(\theta=0)=2\eta\Lambda\chi(\delta_h-\delta_\ell)(\mathcal{V}_h-\mathcal{U}_h),\ \mathcal{P}(\theta=1)=2\eta\Lambda\chi(\delta_h-\delta_\ell)(\mathcal{V}_\ell-\mathcal{U}_\ell),\text{ and}$$

$$\mathcal{P}'(\theta)=\frac{8\alpha\beta\eta^2\Lambda^2\chi^3\left(\delta_h-\delta_\ell\right)^2\left((1-\theta)\delta_h+\theta\delta_\ell\right)(\alpha\gamma-\beta\Lambda+\gamma\eta)}{\left(\rho^2+4\beta\eta\Lambda\left(\alpha+\delta_h(\chi-\theta\chi)+\theta\chi\delta_\ell\right)\right)^{3/2}}.$$

Note that the sign of $\mathcal{P}'(\theta)$ only depends on the sign of $(\alpha\gamma-\beta\Lambda+\gamma\eta)$ because both the denominator of $\mathcal{P}'(\theta)$ and $8\alpha\beta\eta^2\Lambda^2\chi^3\left(\delta_h-\delta_\ell\right)^2\left((1-\theta)\delta_h+\theta\delta_\ell\right)$ are all greater than 0. We, therefore, consider the following cases:

Case 1: If $\beta\Lambda<\alpha\gamma+\gamma\eta$, then $\mathcal{P}(\theta)$ monotonically increases.

Case 2: If $\beta\Lambda=\alpha\gamma+\gamma\eta$, then $\mathcal{P}(\theta)$ is a constant.

Case 3: If $\beta\Lambda>\alpha\gamma+\gamma\eta$, then $\mathcal{P}(\theta)$ monotonically decreases.

From the above three cases, we know that $\mathcal{D}_D^{'m}(\theta)=0$ has at most one solution when $\beta\Lambda\neq\alpha\gamma+\gamma\eta$.

Next, we analyze each of the above cases.

Case 1. When $\beta\Lambda<\alpha\gamma+\gamma\eta$, we first define

$$\mathcal{A}=\alpha(\alpha+\gamma+\eta),\quad \mathcal{C}=\beta\Lambda(\eta-\alpha)+\alpha(\alpha+\eta)(\alpha+\gamma+\eta),$$
$$\mathcal{E}=\sqrt{\alpha^2(\alpha+\gamma+\eta)^2-2\alpha\beta\Lambda(\alpha+\gamma-\eta)+\beta^2\Lambda^2+\chi\delta_\ell\left(2\beta\Lambda(\eta-\alpha)+2\alpha(\alpha+\eta)(\alpha+\gamma+\eta)+\chi(\alpha+\eta)^2\delta_\ell\right)},$$
$$\begin{aligned}\mathcal{F}&=\chi\delta_\ell\left(2\beta\Lambda(\eta-\alpha)+2\alpha(\alpha+\eta)(\alpha+\gamma+\eta)+\chi\delta_\ell((\alpha+\eta)(\alpha+\gamma+\eta)-\beta\Lambda)\right)\\&=\chi\delta_\ell\left(2\mathcal{C}+\chi\delta_\ell((\alpha+\eta)(\alpha+\gamma+\eta)-\beta\Lambda)\right).\end{aligned}$$

Note that $\mathcal{C}>0$ because $\mathcal{C}>(\alpha\gamma+\gamma\eta)(\eta-\alpha)+\alpha(\alpha+\eta)(\alpha+\gamma+\eta)=(\alpha+\eta)\left(\alpha^2+\alpha\eta+\gamma\eta\right)>0$ when $\alpha>\eta$ and $\mathcal{C}$ must be more than 0 when $\alpha\leq\eta$. Additionally, we have $\mathcal{F}>0$ because

$$\mathcal{F}>\chi\delta_\ell\left(2\mathcal{C}+\chi\delta_\ell((\alpha+\eta)(\alpha+\gamma+\eta)-\gamma(\alpha+\eta))\right)=\chi\delta_\ell\left(2\mathcal{C}+\chi\delta_\ell(\alpha+\eta)^2\right)>0.$$

Next, we have

$$\mathcal{V}_\ell-\mathcal{U}_\ell=\frac{-(\mathcal{A}-\beta\Lambda)^2+(\beta\Lambda-\mathcal{A})\mathcal{E}-\chi\delta_\ell\mathcal{C}-4\alpha\beta\Lambda\eta}{\sqrt{(\alpha(\alpha+\gamma+\eta)-\beta\Lambda+\chi(\alpha+\eta)\delta_\ell)^2+4\beta\eta\Lambda\left(\alpha+\chi\delta_\ell\right)}}.$$

Since $-(\mathcal{A}-\beta\Lambda)^2-\chi\delta_\ell\mathcal{C}-4\alpha\beta\Lambda\eta<0$ and

$$\begin{aligned}&\left(-(\mathcal{A}-\beta\Lambda)^2-\chi\delta_\ell\mathcal{C}-4\alpha\beta\Lambda\eta\right)^2-\left((\beta\Lambda-\mathcal{A})\mathcal{E}\right)^2\\=&4\alpha\beta\eta\Lambda\left(\alpha^2(\alpha+\gamma+\eta)^2-2\alpha\beta\Lambda(\alpha+\gamma-\eta)+\beta^2\Lambda^2+\mathcal{F}\right)\\=&4\alpha\beta\eta\Lambda\left(\alpha^2(\alpha+\gamma+\eta)^2-2\alpha\beta\Lambda(\alpha+\gamma+\eta)+\beta^2\Lambda^2+4\alpha\beta\Lambda\eta+\mathcal{F}\right)\\=&4\alpha\beta\eta\Lambda\left((\mathcal{A}-\beta\Lambda)^2+4\alpha\beta\Lambda\eta+\mathcal{F}\right)>0,\end{aligned}$$

we obtain that $\mathcal{V}_\ell-\mathcal{U}_\ell<0$ and thus, $\mathcal{P}(\theta=1)<0$. Consequently, $\mathcal{D}_D^{'m}(\theta)<0$ and $\theta^*=1$.

Case 2: When $\beta\Lambda=\alpha\gamma+\gamma\eta$, then $P(\theta)$ can be reduced to

$$\mathcal{P}(\theta)=-4\eta\Lambda\chi(\alpha+\eta)\alpha\left(\delta_h-\delta_\ell\right)<0.$$

Thus, $\mathcal{D}_D^{'m}(\theta)<0$ and $\theta^*=1$.

Case 3: When $\beta\Lambda>\alpha\gamma+\gamma\eta$:

Case 3.1: When $\mathcal{P}(\theta=1)\geq0$ (i.e., $\mathcal{V}_\ell\geq\mathcal{U}_\ell$), then $\mathcal{P}(\theta)\geq0$ for $\theta\in[0,1]$. Thus, $\mathcal{D}_D^{'m}(\theta)\geq0$ and $\theta^*=0$.

Case 3.2: When $\mathcal{P}(\theta=0)>0$ and $\mathcal{P}(\theta=1)<0$ (i.e., $\mathcal{V}_\ell<\mathcal{U}_\ell$ and $\mathcal{V}_h>\mathcal{U}_h$), then $\mathcal{P}(\theta)$ has a unique root between 0 and 1, which means that $\mathcal{D}_M^m(\theta)$ first increases and then decrease over the interval $[0,1]$. Thus, $\theta^*=\arg\min_{\theta\in\{0,1\}}\mathcal{D}_M^m(\theta)$ considering that the optimal solution can only exist on the boundaries. Note that when $\mathcal{D}_M^m(\theta=0)=\mathcal{D}_M^m(\theta=1)$, we set $\theta^*=0$ for convenience.

Case 3.3: When $\mathcal{P}(\theta=0)\leq0$ (i.e., $\mathcal{V}_h\leq\mathcal{U}_h$), then $P(\theta)\leq0$ for $\theta\in[0,1]$. Thus, $\mathcal{D}_D^{'m}(\theta)\leq0$ and $\theta^*=1$.

Collecting the conditions under which $\theta^*=1$ and $\theta^*=0$ yields the desired characterization stated. Q.E.D.

*Proof of Proposition EC.3.1.* In (EC.6.7), we have obtained

$$\mathcal{D}_{D,M}=\frac{2\eta\Lambda((1-\theta)\chi\delta_h+\theta(\Delta+\chi)\delta_\ell)}{-(\theta-1)\chi(\alpha+2\eta)\delta_h+\alpha\left(\alpha-\beta+\gamma+\eta+\Omega_M\right)+\theta(\alpha+2\eta)(\Delta+\chi)\delta_\ell},$$

where

$$\Omega_M=\sqrt{(\bar{\beta}-\beta+\chi(1-\theta)\delta_h+(\chi+\Delta)\theta\delta_\ell)^2+4\beta\eta}.$$

For a fixed $\theta$, we have

$$\mathcal{D}'_{D,M}(\Delta) = \frac{\mathcal{L}(\Delta)}{\Omega_M \left(-(\theta-1)\chi(\alpha+2\eta)\delta_h + \alpha\left(\bar{\beta}-\beta+\Omega_M\right) + \theta(\alpha+2\eta)(\Delta+\chi)\delta_\ell\right)^2},$$

where

$$\mathcal{L}(\Delta) = 2\alpha\eta\theta\Lambda\delta_\ell \left(\theta\chi\delta_h - \chi\delta_h + \Omega_M - \Delta\theta\delta_\ell - \theta\chi\delta_\ell\right)\left(\bar{\beta}-\beta-\theta\chi\delta_h + \chi\delta_h + \Omega_M + \Delta\theta\delta_\ell + \theta\chi\delta_\ell\right).$$

Next, we have

$$\mathcal{L}'(\Delta) = \frac{2\alpha\eta\theta^2\Lambda\delta_\ell^2(\bar{\beta}-\beta)\left(\bar{\beta}-\beta-\theta\chi\delta_h + \chi\delta_h + \Omega_M + \Delta\theta\delta_\ell + \theta\chi\delta_\ell\right)}{\Omega_M}.$$

Note that $\left(\bar{\beta}-\beta-\theta\chi\delta_h + \chi\delta_h + \Omega_M + \Delta\theta\delta_\ell + \theta\chi\delta_\ell\right) > 0$, and thus the sign of $\mathcal{L}'(\Delta)$ only depends on the sign of $(\bar{\beta}-\beta)$. We, therefore, consider the following cases:

Case 1: If $\beta \le \bar{\beta}$, then $\mathcal{L}(\Delta)$ monotonically increases.

Case 2: If $\beta > \bar{\beta}$, then $\mathcal{L}(\Delta)$ monotonically decreases.

From the above two cases, we know that $\mathcal{D}'_{D,M}(\Delta) = 0$ has at most one solution when $\beta \neq \bar{\beta}$. Next, we analyze each of the above cases.

Case 1. When $\beta \le \bar{\beta}$, there are two cases.

Case 1.1. When $\beta < \bar{\beta}$, it is easy to check that $(\theta\chi\delta_h - \chi\delta_h + \Omega_M - \Delta\theta\delta_\ell - \theta\chi\delta_\ell) > 0$. Thus $\mathcal{L}(\Delta) > 0$ and then $\mathcal{D}'_{D,M}(\Delta) > 0$.

Case 1.2. When $\beta = \bar{\beta}$, $\mathcal{L}(\Delta)$ is reduced to $8\alpha\eta^2\theta\Lambda\delta_\ell(\alpha+\gamma+\eta) > 0$. Then $\mathcal{D}'_{D,M}(\Delta) > 0$ .

Thus, when $\beta \le \bar{\beta}$, $\mathcal{D}'_{D,M}(\Delta) > 0$ .

Case 2. When $\beta > \bar{\beta}$, we have

$$\lim_{\Delta\to 0} \mathcal{L}(\Delta) = 2\alpha\eta\theta\Lambda\delta_\ell\mathcal{T}_1\mathcal{T}_3,$$

where

$$\begin{aligned}
\mathcal{T}_1 &= (\theta-1)\chi\delta_h + \mathcal{T}_2 - \theta\chi\delta_\ell,\\
\mathcal{T}_3 &= \bar{\beta}-\beta+\delta_h(\chi-\theta\chi) + \mathcal{T}_2 + \theta\chi\delta_\ell > 0,\\
\mathcal{T}_2 &= \sqrt{(\bar{\beta}-\beta+\chi(1-\theta)\delta_h + \chi\theta\delta_\ell)^2 + 4\beta\eta} > 0.
\end{aligned}$$

There are two cases.

Case 2.1. When $\mathcal{T}_1 \le 0$, $\mathcal{L}(\Delta) < 0$ for $\Delta \in [0, +\infty)$. Thus, $\mathcal{D}'_{D,M}(\Delta) < 0$.

Case 2.2. When $\mathcal{T}_1 > 0$, let $(\theta\chi\delta_h - \chi\delta_h + \Omega_M - \Delta\theta\delta_\ell - \theta\chi\delta_\ell) = 0$, we have a solution

$$\Delta^* = \frac{2\eta(\alpha+\beta+\gamma) + (\alpha-\beta+\gamma)^2 + \eta^2 - 2\chi(\alpha-\beta+\gamma+\eta)\left((\theta-1)\delta_h - \theta\delta_\ell\right)}{2\theta\delta_\ell(\beta-\alpha-\gamma-\eta)} > 0.$$

Note that when $\mathcal{T}_1 > 0$, we have $2\eta(\alpha+\beta+\gamma) + (\alpha-\beta+\gamma)^2 + \eta^2 - 2\chi(\alpha-\beta+\gamma+\eta)\left((\theta-1)\delta_h - \theta\delta_\ell\right) > 0$. This is because we need to ensure that

$$(\mathcal{T}_2)^2 - ((1-\theta)\chi\delta_h + \theta\chi\delta_\ell)^2 > 0 \Rightarrow 2\eta(\alpha+\beta+\gamma) + (\alpha-\beta+\gamma)^2 + \eta^2 - 2\chi(\alpha-\beta+\gamma+\eta)\left((\theta-1)\delta_h - \theta\delta_\ell\right) > 0.$$

Thus, $\mathcal{D}'_{D,M}(\Delta) > 0$ when $\Delta \in (0, \Delta^*]$ and $\mathcal{D}'_{D,M}(\Delta) < 0$ when $\Delta > \Delta^*$.

Q.E.D.

## References

Doleac, J., A. Mukherjee. 2022. The effects of naloxone access laws on opioid abuse, mortality, and crime. *The Journal of Law and Economics*, 65 (2), 211-238.

Mattson, C. L. 2021. Trends and geographic patterns in drug and synthetic opioid overdose deaths—United States, 2013–2019. *MMWR. Morbidity and Mortality Weekly Report*, 70.

Keyes, K., C. Rutherford, A. Hamilton, J. Barocas, K. Gelberg, P. Mueller, D. Feaster, N. El-Bassel, M. Cerda. 2022. What is the prevalence of and trend in OUD in the United States from 2010 to 2019? Using multiplier approaches to estimate prevalence for an unknown population size. *Drug and Alcohol Dependence Reports*, 3 100052.

Janssen, T., B. R. Garner, J. Yermash, K. R. Yap, S. J. Becker. 2023. Early COVID-related pandemic impacts and subsequent opioid outcomes among persons receiving medication for opioid use disorder: A secondary data analysis of a Type-3 hybrid trial. *Addiction Science & Clinical Practice*, 18 54.